Impact of assimilating satellite and glider observations on Hurricane Isaias (2020) forecast using marine JEDI

[a] Ling Liu, [b] Avichal Mehra, [b] Daryl Kleist, [b] Guillaume Vernieres, [c] Travis Sluka, [c] Kriti Bhargava, [c] Patrick Stegmann, [d] Hyun-Sook Kim, [e] Shastri Paturi, [f]Jiangtao Xu, [f] Ilya Rivin

[a] Ocean Associates Inc, *Silver Spring, MD*

[b] NOAA/NWS/NCEP/EMC, *College Park, MD*

[c] Joint Center for Satellite Data Assimilation (JCSDA), *College Park, MD*

[d] NOAA/AOML, *Key Biscayne, FL*

[e] Axiom Consultants, Inc., *Rockville, MD*

[f] NOAA/NOS/CO-OPS, *Silver Spring, MD*

Corresponding author: Ling Liu, ling.liu@noaa.gov

Early Online Release: This preliminary version has been accepted for publication in *Weather and Forecasting*, may be fully cited, and has been assigned DOI 10.1175/WAF-D-22-0014.1. The final typeset copyedited article will replace the EOR at the above DOI when it is published.

ABSTRACT

Realistic ocean initial conditions are essential for coupled hurricane forecasts. This study focuses on the impact of assimilating high-resolution ocean observations for initialization of the Modular Ocean Model (MOM6) in a coupled configuration with the Hurricane Analysis and Forecast System (HAFS). Based on the Joint Effort for Data Assimilation Integration (JEDI) framework, numerical experiments were performed for the Hurricane Isaias (2020) case, a Category One hurricane, with use of underwater glider data sets and satellite observations. Assimilation of ocean glider data together with satellite observations provides opportunity to further advance understanding of ocean conditions and air-sea interactions in coupled model initialization and Hurricane forecast systems. This comprehensive data assimilation approach has led to a more accurate prediction of the salinity-induced barrier layer thickness that suppresses vertical mixing and sea surface temperature cooling during the storm. Increased barrier layer thickness enhances ocean enthalpy flux into the lower atmosphere and potentially increases tropical cyclone intensity. Assimilation of satellite observations demonstrates improvement in Hurricane Isaias' intensity forecast. Assimilating glider observations with broad spatial and temporal coverage along Isaias' track in addition to satellite observations further increase Isaias' intensity forecast. Overall this case study demonstrates the importance of assimilating comprehensive marine observations to a more robust ocean and hurricane forecast under a unified JEDI-HAFS hurricane forecast system.

SIGNIFICANCE STATEMENT

This is the first comprehensive study of marine observations' impact on hurricane forecast using marine JEDI. This study found that assimilating satellite observations increases upper-ocean stratification during pre-storm of Isaias. Assimilating pre-processed observations from six gliders increases salinity-induced upper ocean barrier layer thickness which reduces sea surface temperature cooling and increases enthalpy flux during the storm. This mechanism eventually enhances hurricane intensity forecast. Overall this study demonstrates a positive impact of assimilating comprehensive marine observations to a successful ocean and hurricane forecast under a unified JEDI-HAFS hurricane forecast system.

1. Introduction

Accepted for publication in *Weather and Forecasting*. DOI 10.1175/WAF-D-22-0014.1.

On July 29 2020, tropical storm Isaias entered the Caribbean Sea as a potential tropical cyclone and made landfall over the Dominican Republic on July 30. Featuring high winds and storm surge, Isaias intensified to a Category One Hurricane on July 31 with a peak surface wind speed of 70 kts while moving across the Bahamas Island. The combination of reduced humidity and increased wind shear weakened Isaias back to a Tropical Storm on August 1. Afterwards Isaias turned north off the coast of Florida and intensified back to a Category One Hurricane at Ocean Isle Beach, North Carolina on 4 August (Figure 1). Hurricane Isaias changes phases between Tropical Storm and Category One hurricane multiple times and it is a relatively large storm (37-40km radius) with an intermediate forward speed (average 5m/s) on its passing area (National Weather Service: Hurricane Isaias 2020).

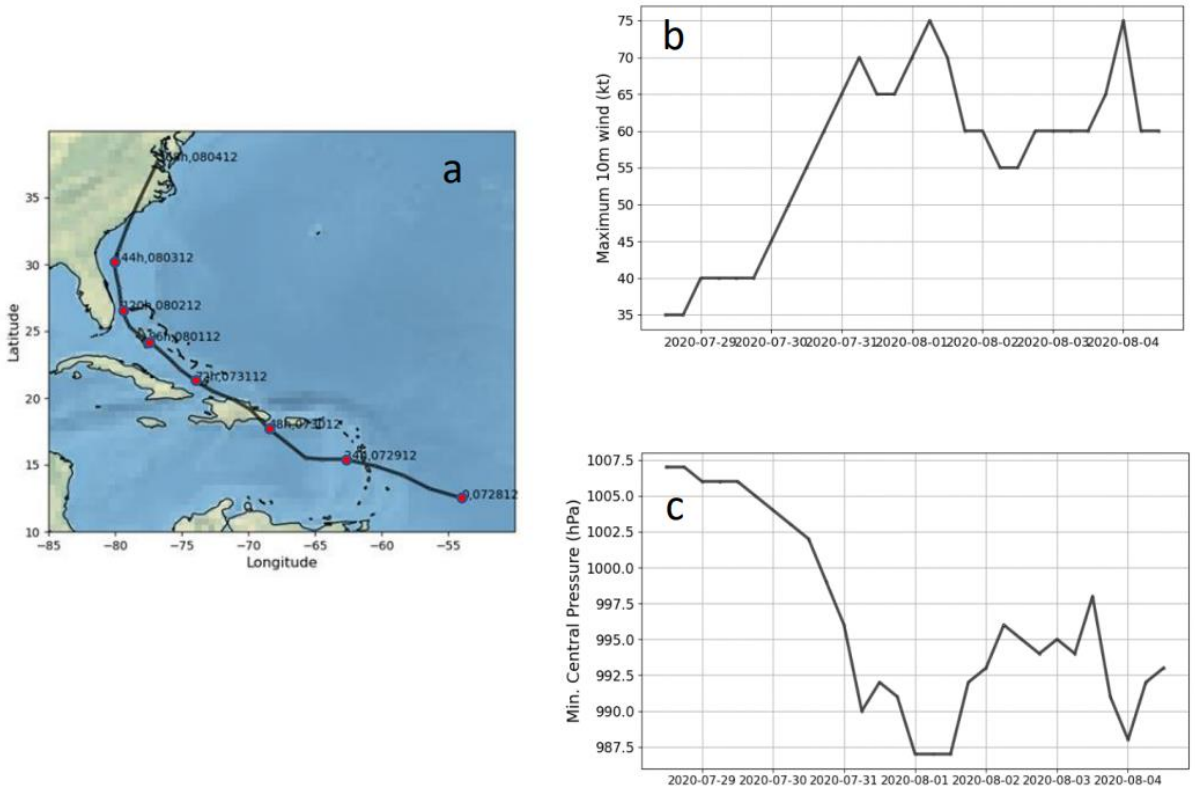

Figure 1. Hurricane Isaias (2020) (a) hurricane track; (b) maximum 10m wind; (c) minimum central pressure between 1200 UTC 28 July and 1200 UTC 4 August 2020.

Hurricane Isaias has caused 17 storm-related deaths and 4.73 billion (2020 USD) in damage occurring in the U.S. alone, making Isaias the costliest hurricane since Hurricane Sandy in 2012 (Wikipedia article on Hurricane Isaias). Hurricanes in general are one of the

File generated with AMS Word template 2.0

Accepted for publication in *Weather and Forecasting*. DOI 10.1175/WAF-D-22-0014.1.

most destructive natural disasters that recur most frequently. In the past they have caused tremendous damage to global life and property (Pielke et al. 2003). Although there are significant improvements in hurricane track prediction with the help of remote sensing technology, large uncertainty still exists in hurricane intensity forecast (Emanuel et al. 2004). Previous studies have documented ocean's control effect on hurricane intensity, especially sea surface temperature changes caused by storm-induced vertical mixing (Lioyd and Vechi, 2011). In order to improve hurricane intensity forecast, it is critical to understand the upper ocean's response mechanism to hurricane intensification.

The initialization of hurricanes usually takes place over the warm surface water of tropical oceans, where the energy is transported from the warm water to the colder atmosphere. Hurricanes, on the other hand, also cause significant sea surface cooling that in turn suppresses their intensity. The hurricane induced SST cooling depends on the mixing layer depth, vertical stratification, air-sea interface heat flux and surface wind speed. The mixed layer is usually defined as the layer with uniform density or temperature (Kara et al. 2003). In the areas with large storm water discharge, the depth of uniform temperature layer surpasses uniform density layer. This difference creates a barrier layer (BL) that suppresses vertical mixing and cooling during the storm (Sprintall and Tomczak 1992).

Coupled high-resolution ocean and atmospheric models provide an essential tool to help understand the ocean's response to strong atmospheric forcing. Here a combination of glider, satellite and modeled dataset are used to quantify the impact of barrier layers on hurricane Isaias' intensification through calculation of the SSTs change, enthalpy flux and intensification statistics, as well as their relationships with barrier layer thickness (BLT). The surface temperature of the ocean plays an important role to the formation and cooling of the tropical cyclone. A warm ocean surface also intensifies the hurricane by providing an upper-ocean heat potential, which is the integrated heat content from the surface down to the 26ºC isotherm depth (Leipper et al. 1972). The 26ºC isotherm depth is an important indicator of Tropical Cyclone Heat Potential (TCHP), defined as the energy needed for a Tropical Cyclone (TC) to raise temperature above 26ºC (Goni et al. 2009). Heat content plays a more important role of sustaining the hurricane than just sea surface temperature alone (Prasad and Hogan 2007).

While wind induced upwelling and turbulent mixing disperse hurricane energy and cause strong sea surface cooling, baroclinic processes within the thermocline adjust this process

Accepted for publication in *Weather and Forecasting*. DOI 10.1175/WAF-D-22-0014.1.

through internal wave dispersion within a barrier layer featuring low salinity from freshwater discharge. The barrier layer acts against sea surface cooling by creating strong stratification that dampens vertical mixing (Domingues et al. 2015). However, the situation reverses when vertical shear from strong wind mixing dominates stratification caused by freshwater input. The barrier layer often leads to strong sea surface cooling over strongly stratified underlying water as shown by Glenn et al. 2016. The pre-existing upper ocean dynamics makes a big difference on how the ocean reacts to hurricanes and thus leads to different storm features. Understanding the initial temperature and salinity structures in the upper ocean is the key to learn how the phase changes of a hurricane occur.

Compared to extensive modeling studies based on hurricane theories, hurricane marine observations are limited due to obvious operational difficulties. Conventional hurricane observations including moorings can record upper water column variations at fixed locations. However, upper ocean response to hurricanes is active and four dimensional, so using such observations alone is insufficient. Satellite derived observations from altimeters and microwave instruments such as Absolute Dynamic Topography (ADT) and SST are capable of resolving the surface but not vertical variations in the upper ocean. Underwater hurricane gliders repeatedly observing vertical transects at flexible locations especially along hurricane tracks may help identify the barrier layers and resolve rapid upper ocean responses to hurricanes (Oke et al. 2009). Assimilating glider data has also shown to improve simulated sub-surface velocity correlation to the observations as well as thermocline circulation (Mourre and Chiggiato 2014; Testor et al. 2019). Kurapov et al. 2018 demonstrated that assimilating glider data together with the surface observations could improve ocean forecast whereas assimilating glider data alone without constraint from surface observations might increase spurious error variability.

The impact of assimilating different marine observations to hurricane intensity forecast depends on the relationship between hurricane intensity and SSTs changes. However, there is a lack of quantitative understanding about this relationship. Dong et al. 2017 presented a case study of Category 4 Hurricane Gonzalo and hypothesized that little impact of assimilating glider data over Gonzalo's intensity forecast was possibly caused by the insensitivity of a relatively small hurricane (27 km diameter) with large heat potential (> 85KJ cm-2) to the sea surface temperature changes brought by assimilating localized glider observations. However, the 2017 study did not explore the physical mechanism that potentially led to this hypothesis.

Accepted for publication in *Weather and Forecasting*. DOI 10.1175/WAF-D-22-0014.1.

Halliwell et al. 2015 found that enthalpy flux during hurricane intensification adjusts primarily to 10-m temperature and humidity; secondarily to surface wind. Although the 2015 study addressed the role of TCHPs in regulating the enthalpy flux, it did not examine the role of the upper ocean stratification to its adjustment to surface wind and temperature which has a direct impact on hurricane's intensification.

In order to address these limitations, this study first presents a very unique hurricane case study, a hurricane with large radius of impact that went through multiple phase changes between a tropical storm and a Category 1 hurricane during its life cycle. It then investigates the impact of initializing SSTs through assimilating satellite observations and underwater glider data from NOAA's Atlantic Oceanographic and Meteorological Laboratory (AOML) on the ocean initial condition during the hurricane. In this case study, the characteristic of ocean barrier layer (BL) and its impact on the upper ocean stratification are analyzed on both sides of the hurricane track. The barrier layer thicknesses (BLTs) derived from different ocean initial conditions are calculated and compared in order to identify the mechanism leading to different enthalpy flux exchanges, which have a direct impact on hurricane's intensification. At last, the sensitivity of hurricane intensity forecasts to assimilating different marine observations are assessed as a result of this mechanism.

The study applies the Modular Ocean Model (MOM6) at HAT10 (i.e., a basin covering the North Atlantic Ocean [1^{o}N, 45.78^{o}N], [100^{o}W, 10^{o}E]) in a coupled configuration with the Hurricane Analysis and Forecast System (HAFS) using the Joint Effort for Data Assimilation Integration (JEDI) infrastructure (Figure 2). HAFS is planned to become the next-generation multi-scale numerical model for hurricane prediction based on NOAA's Unified Forecast System (UFS) and JEDI framework. This is not only the first study that investigates the impact of the ocean observations with the coupled atmosphere and ocean models using the UFS infrastructure software: Community Mediator for Earth Prediction Systems (CMEPS), but also the first study that engages both the UFS and the multi-scale DA system with continuous cycling using the new marine JEDI system.

Accepted for publication in *Weather and Forecasting*. DOI 10.1175/WAF-D-22-0014.1.

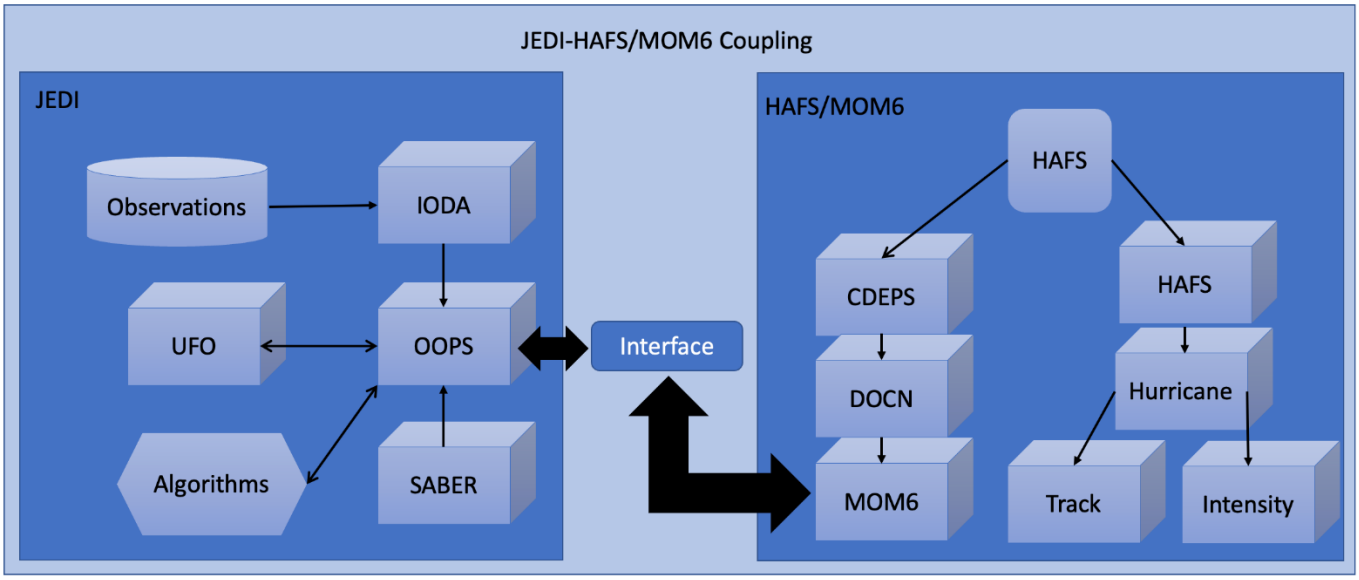

Figure 2. Flow chart of JEDI/HAFS coupling.

The forecast period of this study is from 1200 UTC 28 July to 1200 UTC 2 August 2020 (120 hours), during which Isaias intensified to a Category One Hurricane, made landfall at Dominican Republic Island, and then almost weakened to a tropical storm before strengthened into a Category One Hurricane again. Isaias relaxed back into a tropical storm until the end of the forecast period of this study (Figure 1b). The manuscript is organized as follows: Section 2 describes the marine observations and experiment configurations; Section 3 evaluates the impact of marine observations on ocean initial condition and ocean observations' impact on ocean barrier layers; the impacts on ocean and hurricane forecasts are discussed in Section 4; Section 5 provides summary of this study.

2. Marine observations and experiment designs

a. Marine observations for data assimilation and validation

The marine observations assimilated in this study are Absolute Dynamic Topography (ADT) data derived from satellites including Envisat, TOPEX/Poseidon, Jason-1 and OSTM/Jason-2; Sea Surface Temperature (SST) data measured by the Advanced Microwave Scanning Radiometer 2 (AMSR2); SST data obtained from the Global Precipitation Measurement (GPM) Microwave Imager (GMI); ACSPO Global SST data derived from the Suomi NPP Visible Infrared Imaging Radiometer Suite (VIIRS); the SST product from the WindSat Polarimetric Radiometer. The observation errors of the above satellite data assimilated on 28 July 2020 are shown by Figure 3. For ADT data configuration, the

File generated with AMS Word template 2.0

Accepted for publication in *Weather and Forecasting*. DOI 10.1175/WAF-D-22-0014.1.

observation errors are set to have absolute threshold of 0.2m. Regarding the determination of representative error, please refer to the observation error algorithm in the JEDI documentation.

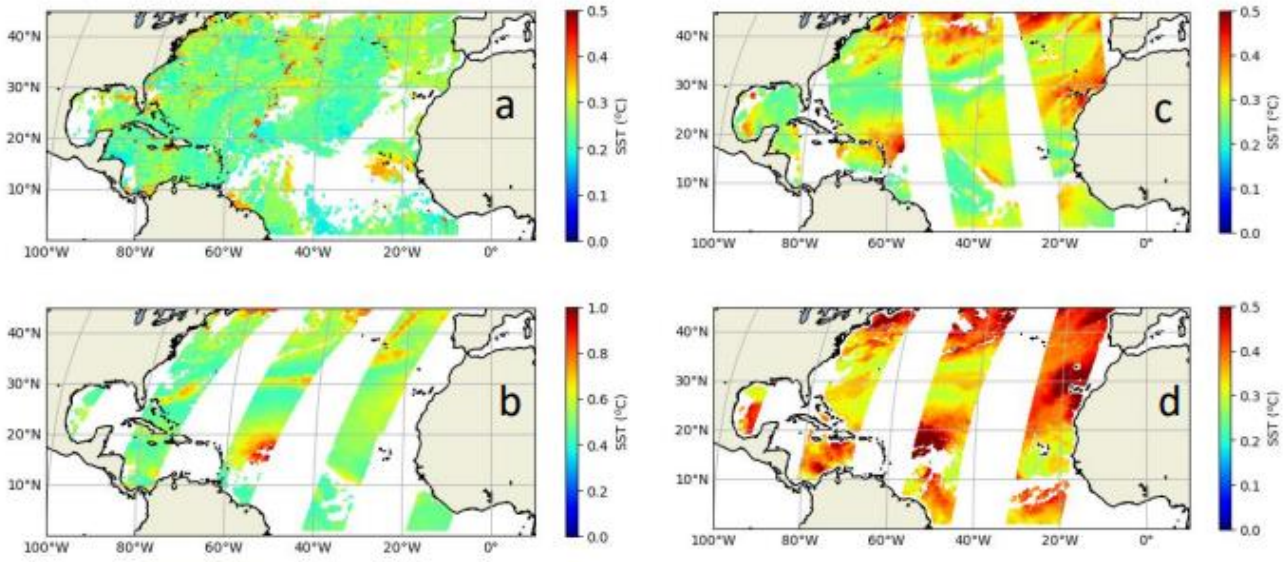

Figure 3. Instrumental errors of SSTs (°C) measured by (a) VIIRS; (b) GMI; (c) AMSR2; (d) Windsat assimilated in marine JEDI on 28 July 2020.

In addition to the satellite observations, six gliders named as SG663, SG649, SG664 and SG669, SG609, SG665 piloted near Puerto Rico Island between the surface and 1000 meters depth deployed by AOML between 20 July and 6 August 2020 are also assimilated into marine JEDI. The track of each of the six gliders assimilated between 20 July and 6 August 2020 are shown by Figure 4. The observation error of the AOML glider data is set to 0.2°C for temperature based on the observation and JEDI representation error calculation. Number of observations assimilated on 28 July 2020 in marine JEDI within HAT10 model domain are listed in Table 1.

Accepted for publication in *Weather and Forecasting*. DOI 10.1175/WAF-D-22-0014.1.

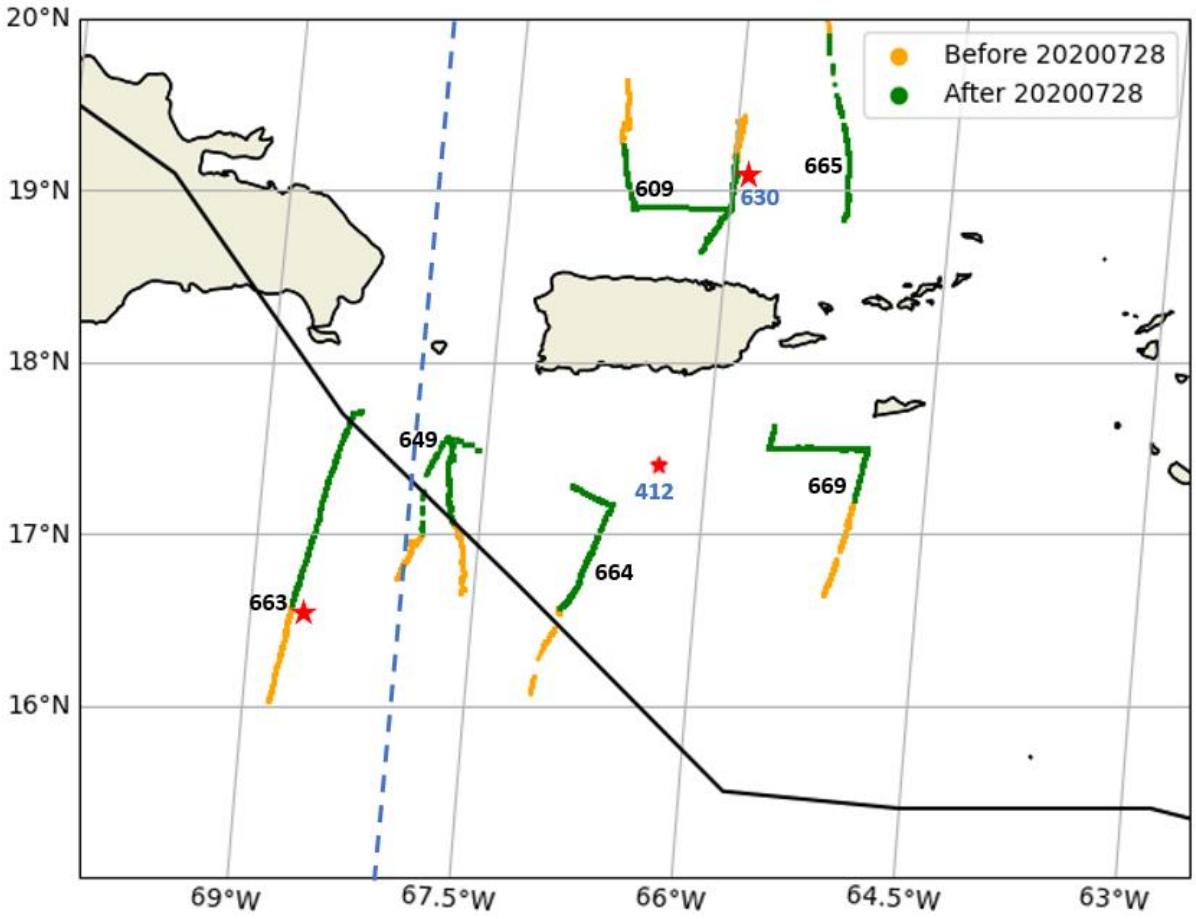

Figure 4. Six AOML Glider data tracks assimilated between 1200 UTC July 20 and 1200 UTC 6 August 2020 (Orange color shows data assimilated before 20200728; Green color are the data assimilated after 20200728). The location of glider NG412 (RUCOOL), SG663 and SG630 are shown by the red stars. Black line indicates hurricane track. Blue dashed line indicates the location of the 68°W vertical section.

Instruments	Altimetry	AOML glider (profiles, thinning applied)	AMSR2 SST	GMI SST	Viirs SST	Windsat SST
nobs	25463	7115	69040	23930	256022	19292

Table 1. Number of observations assimilated on 28 July 2020 in marine JEDI within HAT10 model domain.

There are approximately 25000 AOML glider measurements during each day of the data assimilation experiment period. In order to enhance calculation efficiency, reduce

File generated with AMS Word template 2.0

Accepted for publication in *Weather and Forecasting*. DOI 10.1175/WAF-D-22-0014.1.

computational cost and overfitting, thinning box with 1-degree horizontal length and 10m vertical length is applied to filter through the glider data. Number of glider observations at each MOM6 layer depth on July 28, 2020 before and after thinning are compared in Figure 5. Only the thinned glider data are used in the data assimilation experiments. Additional AOML underwater glider data SG630 and NG412 obtained by Rutgers University Center for Ocean Observing Leadership (RUCOOL) are used as independent validation datasets. The locations of the three validation gliders on 28 July are shown by Figure 4.

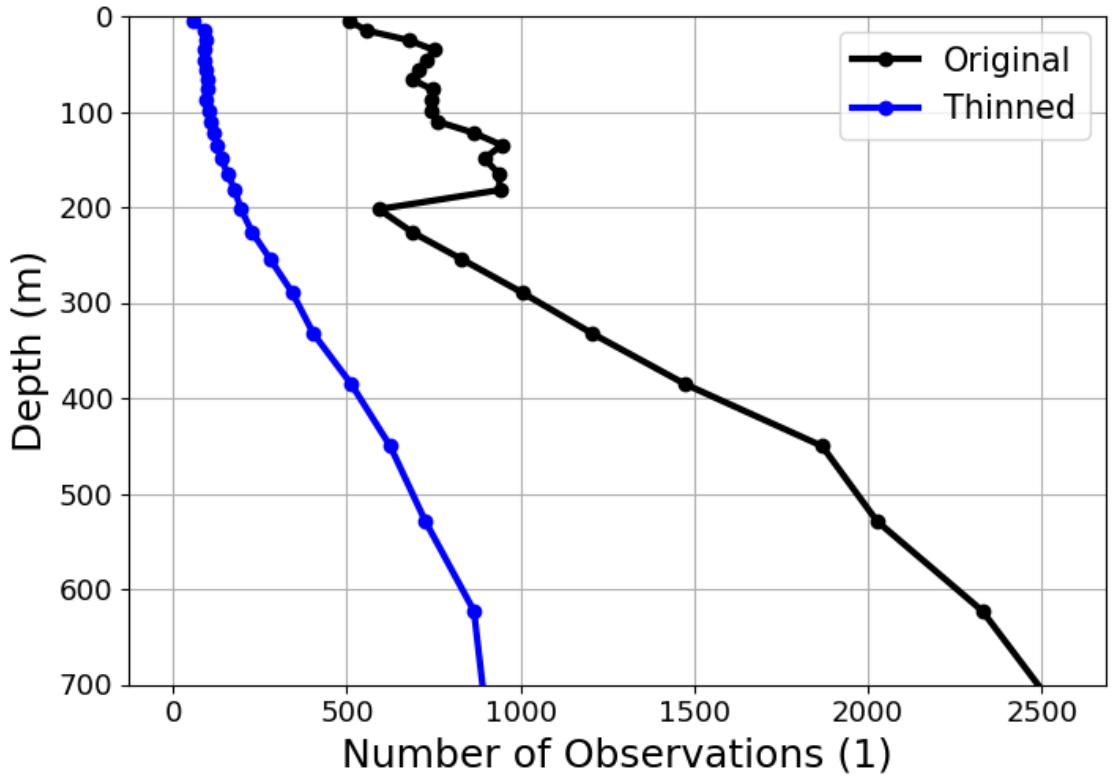

Figure 5. Number of glider observations at each MOM6 layer before and after thinning.

b. Model and Experiments setup

1) Marine JEDI

Marine JEDI is the marine data assimilation system for MOM6 based on the JEDI development at the Joint Center for Satellite Data Assimilation (JCSDA) and the Environmental Modeling Center (EMC)/National Centers for Environmental Prediction (NCEP) (Trémolet and Auligné 2020). The interface between MOM6 and JEDI is developed under the Sea-ice Ocean Coupled Assimilation Project (SOCA). The data assimilation system

Accepted for publication in *Weather and Forecasting*. DOI 10.1175/WAF-D-22-0014.1.

SOCA is based on the JEDI infrastructure for its unified and versatile capability for Earth System Prediction (JEDI documentation). The part of SOCA applied in this study is an incremental 3DVAR assimilating potential temperature and practical salinity profiles (Courtier et al. 1998). In this approach, 3D-Var minimizes the objective function J

$$J(\delta x) = \frac{1}{2}\delta x^k B^{-1}\delta x + \frac{1}{2}(H\delta x - d)^T R^{-1}(H\delta x - d), \quad (1)$$

Where

$$B = KDFF^T D^T K^T, \quad (2)$$

B stands for the background error covariance matrix, or static B-matrix. K is the linearized balance operator that establishes the multivariate background-error covariances. D is the diagonal matrix that contains the standard deviation of errors for temperature and salinity. FF^T can be interpreted as a correlation matrix, in which the horizontal length scale is scaled by the Rossby radius of deformation that has a minimum value of 50 km and a maximum value of 200 km based on (Chelton et al. 1998).

2) The coupling between MOM6 and HAFS

The hurricane model applied in this study is the Hurricane Analysis and Forecast System (HAFS). It is the hurricane application for the Unified Forecast System (UFS) and uses FV3 (Finite Volume Cubed Sphere Dynamical Core) based multi-scale model with data assimilation that was capable of hurricane track and intensity analyses and 120-hour forecasts (https://github.com/hafs-community/HAFS). In this study, the atmospheric FV3 component of HAFS uses a 13 km resolution for the HAFS regional domain, i.e., North Atlantic NATL basin with a 3 km domain resolution and an extended 91 model vertical levels (Liu et al. 2020, Figure 6). HAFS solves nonhydrostatic equations on the rotational horizontal mesh with domain center location at 22ºN, 62ºW and domain size of 2880x1920.

Accepted for publication in *Weather and Forecasting*. DOI 10.1175/WAF-D-22-0014.1.

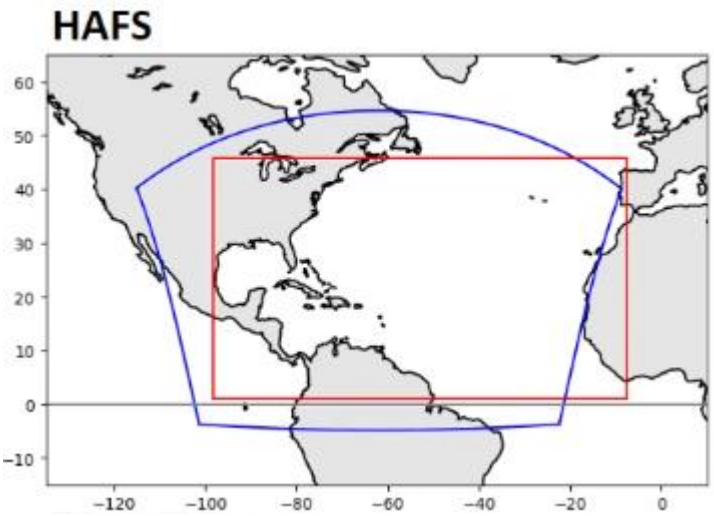

Figure 6. HAFS model domains applied in this study. Blue domain indicates FV3 atmospheric domain for HAFS; Red shows the model domain for the regional MOM6 experiments.

The ocean model MOM6 covers the HAT10 basin ([1^{o}N, 45.78^{o}N], [100^{o}W, 10^{o}E]) at a 1/12-degree resolution with 51 vertical layers (Figure 6). The ocean initial and boundary conditions come from the Real-Time Ocean Forecast System (RTOFS) nowcast, and the lateral boundary condition is the standard oceanic open boundary condition, i.e., the Flather boundary condition for the barotropic component and an Orlanski-type radiation condition for the baroclinic component. Atmospheric forcing is from 0.25-degree resolution GFS forcing. A K-profile parameterization scheme (KPP) was applied as the vertical mixing scheme in MOM6 (Adcroft et al. 2019).

The coupling between HAFS and MOM6 is through the Community Data Models for Earth Prediction Systems (CDEPS documentation). In this coupled system, FV3 based GFS provides MOM6 with a 0.25 degree forcing, while MOM6 provides Sea Surface Temperature (SSTs) to HAFS every 24 hours for 120 hours with the initial condition at 1200 UTC 28 July 2020. The atmospheric model of HAFS is initialized using the GFS analysis at 1200 UTC 28 July 2020. The beginning of the storm is adjusted to the National Hurricane Center best track location. The vortex initialization is implemented for the FV3 component of HAFS according to TC vitals. GFS forecast provides lateral boundary conditions for HAFS (Liu et al. 2020). Only oceanic data assimilation is performed in this study.

3) Data assimilation experiments design

File generated with AMS Word template 2.0

Accepted for publication in *Weather and Forecasting*. DOI 10.1175/WAF-D-22-0014.1.

A free MOM6 experiment without data assimilation initialized using HYbrid Coordinate Ocean Model (HYCOM) background from January to December 2020, named as NODA, is marked as the baseline experiment. In fact, both the model free run and data assimilation experiments have spin-up period between 1 January and 20 July, 2020. The data assimilation period of the three experiments is performed between 20 July and 6 August 2020 at 1200 UTC of each day. The initial condition for hurricane forecast is 1200 UTC 28 July with seven-months model spin-up period and one-week data assimilation spin-up period. The CTRL experiment in this study assimilates the Altimeter Satellite Absolute Dynamic Topography (ADT) products, satellite Sea Surface Temperature. The Glider experiment (GLD) assimilates only AOML glider data. The ALL experiment assimilates AOML glider data and the data that are used by the CTRL experiment. After initializing the ocean model, the updated ocean model background of SSTs derived from the four experiments, i.e., NODA, CTRL, GLD and ALL are applied to the Data Ocean (DOCN) component of CDEPS coupled to HAFS in order to perform the 120-h hurricane forecast with the initial condition on 28 July 2020.

c. Calculation of BLT, enthalpy flux, SST change and hurricane intensification index

The barrier layer thickness (BLT) is calculated as the difference between the bottom of the density mixing layer (MLD) and isothermal layer depth (ILD). In this study the isothermal layer depth is calculated using a 0.8^{o}C temperature change criteria (Kara et al., 2000). Enthalpy flux is evaluated as the sum of latent and sensible heat fluxes derived from HAFS forecast. The hurricane intensification factor is calculated as the linear regression coefficient of the maximum wind speed over six data points with six hours intervals in between (Lioyd et al. 2011). The SST change is derived from HAFS forecast as the SST difference between one day after the forecast period and the average SST during the eight-day period before pre-storm.

3. Impact of marine observations on Hurricane Isaias' ocean initial condition

a. Satellite and glider observations' impact on upper ocean structure

In order to evaluate the impact of assimilating satellite and glider observations on the upper-ocean conditions, the initial conditions of temperature and salinity derived from four

File generated with AMS Word template 2.0

Accepted for publication in *Weather and Forecasting*. DOI 10.1175/WAF-D-22-0014.1.

experiments at 1200 UTC 28 July are interpolated to the RUCOOL verification glider location (17.4ºN, 66.33ºW, Figure 4) and compared to the observed temperature and salinity profiles (Figure 7). The temperature and salinity differences between model outputs and verification glider observations are shown by Figure 8.

The observed initial profile indicates a mixed layer depth of approximately 50m and a surface temperature slightly above 29ºC (Figure 7a). The temperature profile of NODA indicates a 35m mixed layer depth and a negative bias of approximately 0.75ºC compared to the glider profile (Figure 7a and 8a). The cold bias of NODA increases with depth and reaches a local maximum that is greater than 1.5ºC between 52 and 74m. This negative bias decreases to approximately 1.4ºC between 75 and 100m, below which it reaches a value of less than -1.5ºC. The GLD experiment improves the upper-ocean temperature structure by reducing the negative bias to be less than 0.5ºC for the upper 100m water column, which is a larger than 50% of improvement compared to NODA. The CTRL experiment assimilating satellite observations indicates an average of 25% of improvement of bias throughout the water column relative to the NODA (Figure 7a). ALL experiment assimilating glider and satellite observation shows 30% (i.e., $\frac{0.25}{0.75} \cdot 100\%$) of further improvement at the surface in addition to CTRL experiment, implying contribution from assimilating thinned glider data.

The storm-induced low salinity above 25m depth has led to a shallower density mixing layer than the isothermal layer, which forms a barrier layer suppressing sea surface temperature cooling. The barrier layer thickness (BLT) is calculated as the difference between the bottom of the density mixing layer depth (MLD) and isothermal layer depth (ILD). In this study the ILD is calculated using a 0.8ºC temperature change criteria (Kara et al., 2000). Figure 7 shows that the MLD is about 25m deep, the ILD for CTRL and ALL are about 60m and 70m deep, respectively. The BLTs are thus about 35m and 45m deep for CTRL and ALL, respectively. This result indicates that at this location ALL and GLD have deeper ILD than CTRL, which lead to thicker barrier layers (BLs).

Accepted for publication in *Weather and Forecasting*. DOI 10.1175/WAF-D-22-0014.1.

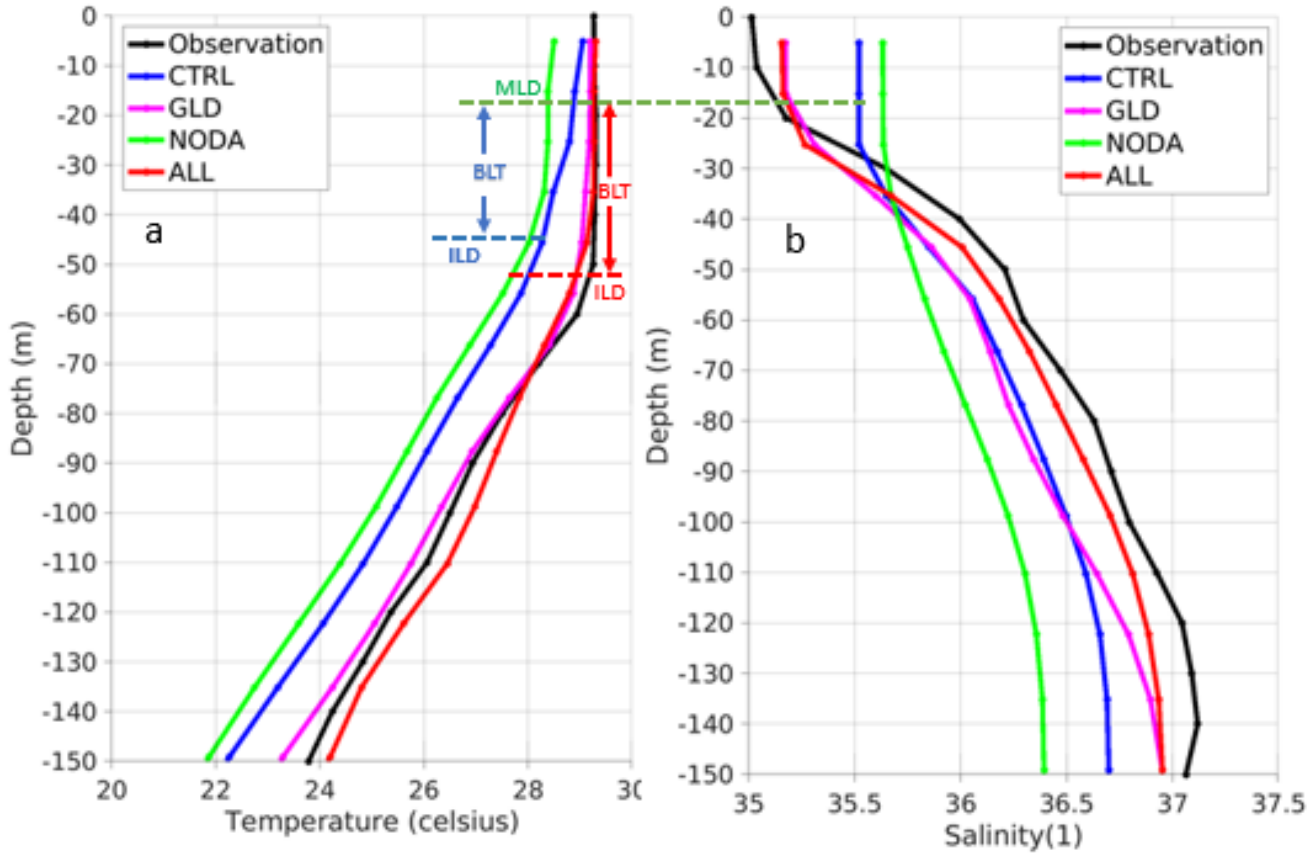

Figure 7. (a) Temperature and (b) Salinity profiles on 28 July 2020 from four experiments compared to RUCOOL Glider observation (NG412).

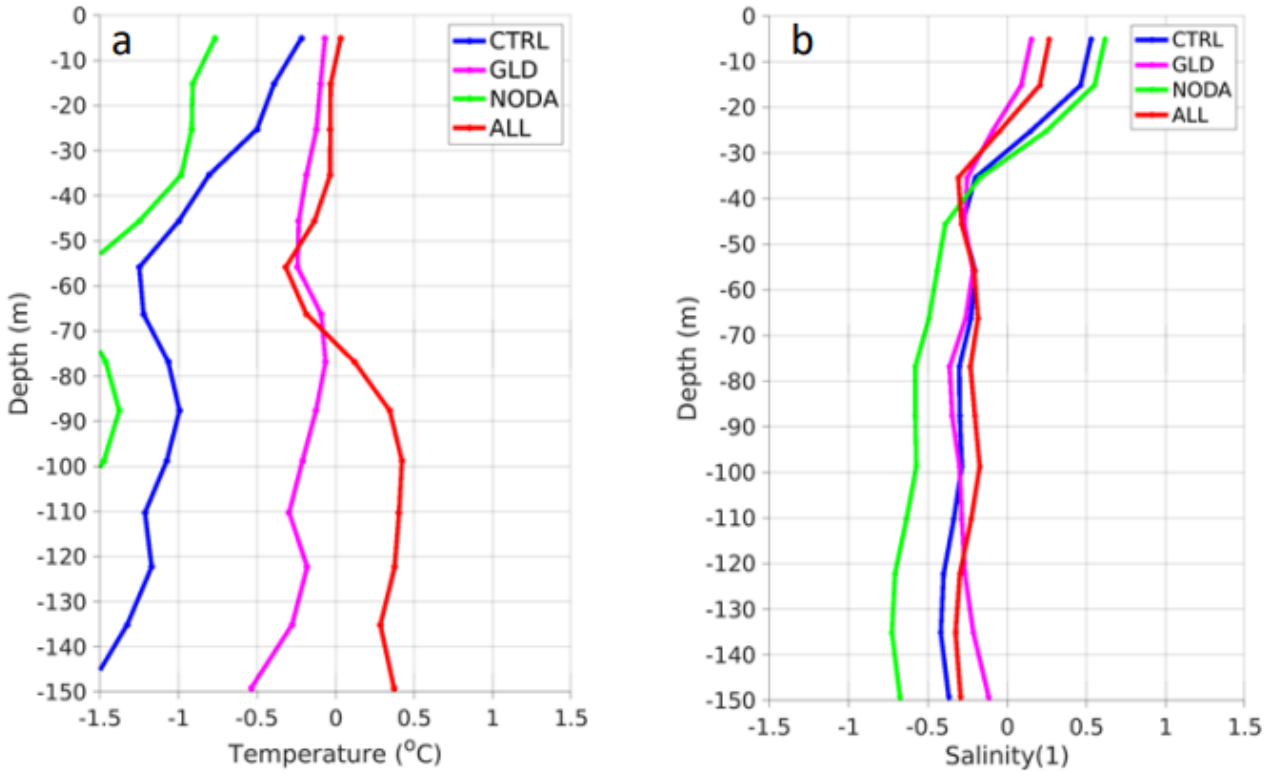

File generated with AMS Word template 2.0

Accepted for publication in *Weather and Forecasting*. DOI 10.1175/WAF-D-22-0014.1.

Figure 8. (a) Temperature and (b) Salinity error profiles of four experiments on 28 July 2020.

The salinity profile is an important factor determining the density structure and vertical stratification of the ocean, which contributes to the formation of barrier layer. The salinity observation collected from the RUCOOL glider indicates a rapid increase from 35 psu at surface to 36.2 psu at 50m. NODA and CTRL at the top 25m water column over-estimate the salinity by 0.5 and 0.6 psu, respectively (Figure 8b). The assimilation of AOML glider data improves the surface salinity error of GLD to 0.15 psu and ALL to approximately 0.23 psu, which is an approximate 30% (i.e., $\frac{0.25\ \text{psu}}{0.75\ \text{psu}} \cdot 100\%$) of improvement compared to NODA at surface. Below 50m, CTRL and ALL reduce their error estimates to approximately 0.25 and 0.3 psu compared to 0.6 psu of NODA, leading to 42% (i.e., $\frac{0.25\ \text{psu}}{0.6\ \text{psu}} \cdot 100\%$) and 50% (i.e., $\frac{0.3}{0.6} \cdot 100\%$) error reductions. There is an 8% of improvement in ALL assimilating both satellite observations and glider data compared to CTRL with only satellite observations assimilated. This difference implies that assimilating glider data improves salinity structure especially when satellite observations are also assimilated.

Below the bottom of the density mixing layer a strong density gradient is indicated by the increased buoyancy frequency (i.e., a measure of the water column stability to vertical displacements) between 25 and 70m (Figure 9b). Among four experiments, ALL captures 83% (i.e., $\frac{2.5\text{x}10^{-4}}{3\text{x}10^{-4}} \cdot 100\%$) of the upper barrier layer and GLD contributes about 66% (i.e., $\frac{2\text{x}10^{-4}}{3\text{x}10^{-4}} \cdot 100\%$). NODA and CTRL are unable to detect the density barrier layer with smoothly increased buoyancy frequency from the surface to 50m depth. With glider data assimilated in addition to satellite observations, ALL indicates the closest density gradient to the observation at 25m depth.

File generated with AMS Word template 2.0

Accepted for publication in *Weather and Forecasting*. DOI 10.1175/WAF-D-22-0014.1.

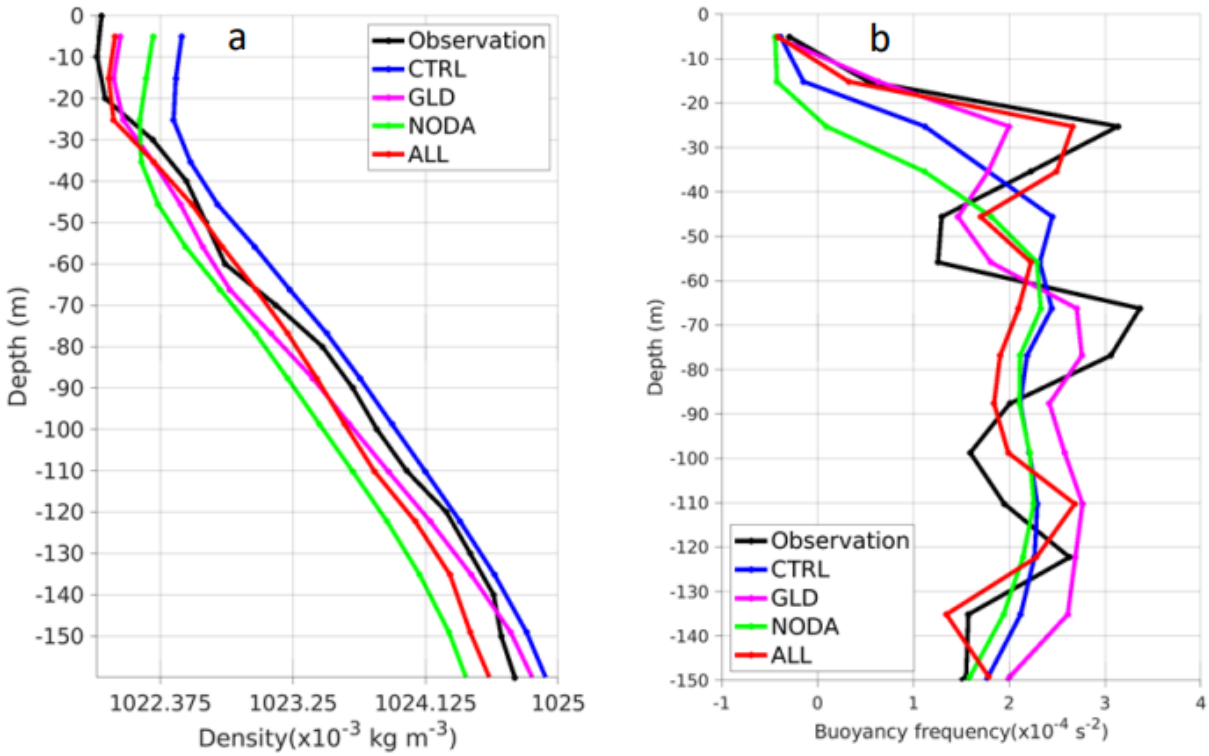

Figure 9. (a) Density and (b) Buoyancy frequency profiles of four experiments compared to RUCOOL glider observation on 28 July 2020.

b. Satellite and glider observations' impact on ocean barrier layer

We have shown that the BLs at Station 412 (RUCOOL) calculated from the observation, ALL and GLD initial conditions are approximately between 25m and 70m depths using a 0.8^{o}C temperature change criteria. The BLTs' spatial distribution and its impact on the SSTs change during the storm are potentially important factors to the storm intensity forecast. We then choose two other validation gliders, namely SG663 and SG630 on July 28, parked on the two sides of the hurricane track (Figure 4) and calculate the BLTs from their measurements (Figure 10 and 11). Figure 10 shows that for SG663 located on the left of the track, the MLD is about 30m deep derived from density/salinity profiles, the ILD for ALL initial condition and the observation is about 60m deep. The BLT at this location is thus about 30m deep. CTRL and NODA initial conditions both underestimate the SST. This result indicates that at this location BLT is thinner than that calculated from NG412 located to the right of the track (Figure 7). On the further right side of the hurricane track to the north of Puerto Rico island, an independent glider SG630 is chosen to compare to four initial conditions at this location

File generated with AMS Word template 2.0

Accepted for publication in *Weather and Forecasting*. DOI 10.1175/WAF-D-22-0014.1.

(Figure 11). While the MLD is about 20m deep, the vertical temperature reduction is more gradual, which leads to a deeper ILD near 70m depth at this location. This results in a thicker BLT (50m) compared to the one located on the left of the track and NG412. Since hurricane induced cooling usually occurs on the right of the hurricane track, this increasing BLT towards the further right of the track might have profound implication to the SST cooling during the storm.

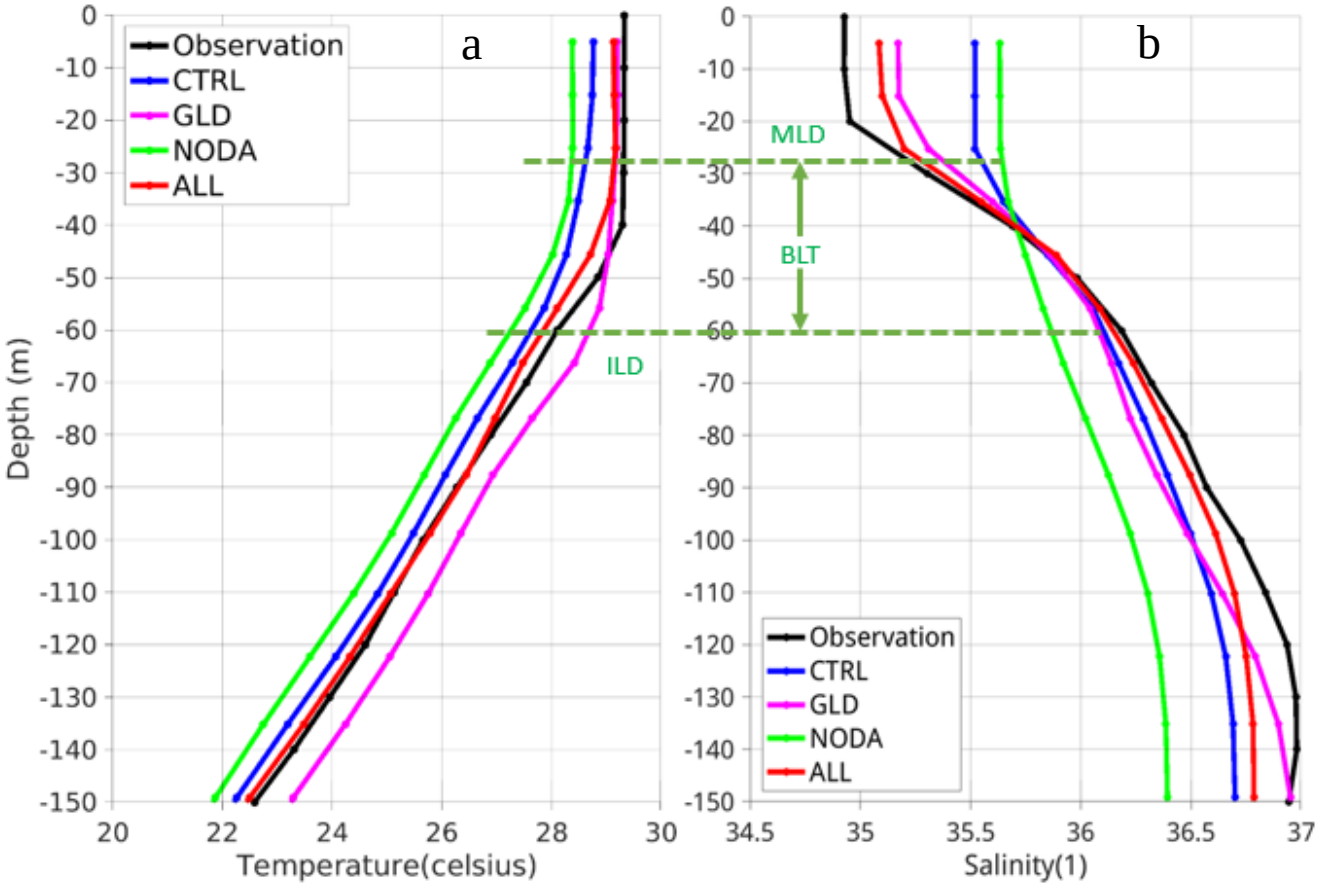

Figure 10. (a) Temperature and (b) Salinity profiles of four experiments on 28 July 2020 compared to observed profile measured by glider SG663, to the left of the hurricane track.

File generated with AMS Word template 2.0

Accepted for publication in *Weather and Forecasting*. DOI 10.1175/WAF-D-22-0014.1.

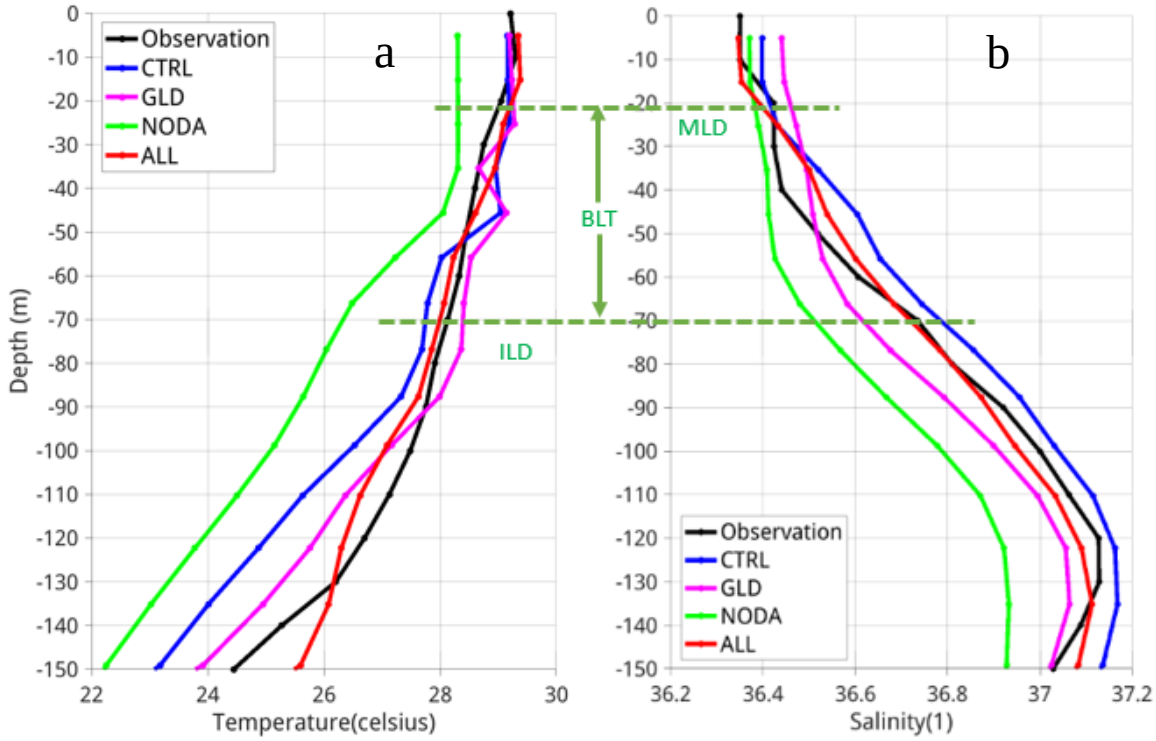

Figure 11. (a) Temperature and (b) Salinity profiles of four experiments on 28 July 2020 compared to observed profile measured by glider SG630, to the right of the hurricane track.

A 68°W latitudinal vertical section across the hurricane track is selected in order to further understand marine data assimilation's role on the meridional variability of the vertical stratification during the pre-storm (Figure 12 and 13). Assimilation of glider data alone increases the depth of mixing layer depth by nearly two folds to the left of the hurricane track (Figure 12b). On the right of the hurricane track the 28°C isotherm deepens when glider data are assimilated (Figure 12b and d). This results in increased BLTs up to 45m (by definition it is the difference between the bottom of the MLD and the 0.8°C temperature change isotherm) in GLD and ALL initial conditions. To the left of the track GLD predicts an inversion of temperature at the scale of 0.5°C near the track between 20m and 80m depths, within which the salinity increases compared to the surface (Figure 13b). For ALL initial condition the inversion layer is between 20 and 45m depths (Figure 12d and 13d), which indicates a shallower MLD. When a storm passes over such ocean condition, the warm saline water within the pycnocline is more likely to get entrained into the mixed layer, resulting in a reduced SST cooling or even warming. CTRL initial condition shows increased BLT (approximately 20-30m) on both sides of the hurricane track than NODA, but not as prominent as GLD and ALL especially to the right of Isaias' track.

File generated with AMS Word template 2.0

Accepted for publication in *Weather and Forecasting*. DOI 10.1175/WAF-D-22-0014.1.

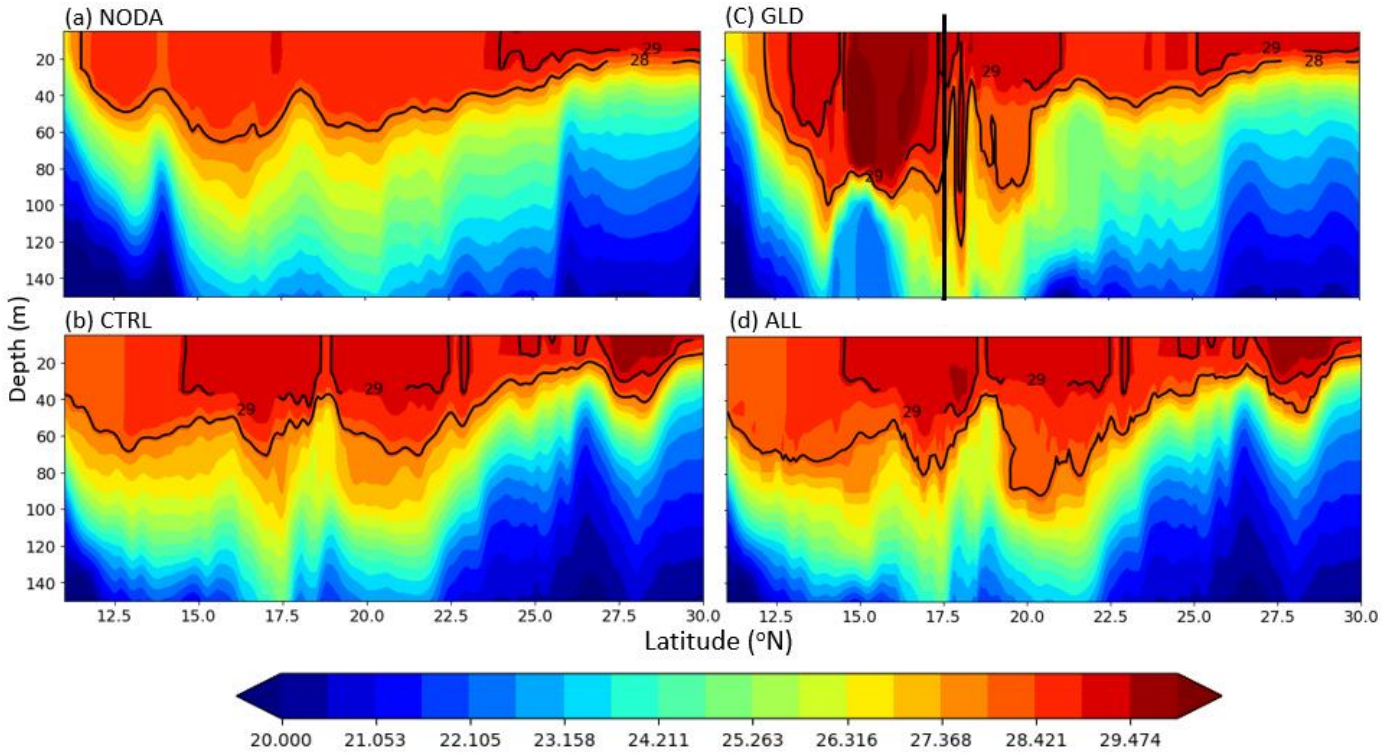

Figure 12. MOM6 Temperature distribution across 68oW latitudinal transection. (a) NODA; (b) GLD; (c) CTRL; (d) ALL. Two contour lines indicate 28oC and 29oC isotherms. Black line in (b) indicates the location of the hurricane track on 28 July 2020.

The 68°W vertical section for the salinity indicates a warm and low-salinity storm water discharge that increases upper ocean stratification and reduces hurricane induced vertical mixing and thus plays an important part for the SSTs warming on the left of the track (Figure 13). Both GLD and ALL initial conditions predict below 35 psu of minimum surface salinity to the left of the hurricane track. NODA and CTRL initial conditions mostly indicate higher than 35 psu surface salinity. On the right of the hurricane track when both glider and satellite observations are assimilated in the ALL initial condition, the surface salinity is mostly increased to above 36.5psu (Figure 13d). This result in combination with increase of BLTs shown by the temperature vertical profile (Figure 12) indicate the vertical entrainment of deep warm saline water below pycnocline to the near surface causing reduced SSTs cooling or even warming. The enhanced upper-ocean stratification caused by surface discharge of warm and fresh storm water to the left of the hurricane track and the increased BLTs through vertical entrainment of deep warm and saline water on the right lead to the pre-storm vertical stratification. The increased stratification on the left of the track leads to further SSTs warming; the increased BLTs on the right of the hurricane track potentially leads to reduced SSTs cooling and even slight warming. Initial conditions without data assimilation, or assimilates only one data source are not able to demonstrate this warming mechanism.

File generated with AMS Word template 2.0

Accepted for publication in *Weather and Forecasting*. DOI 10.1175/WAF-D-22-0014.1.

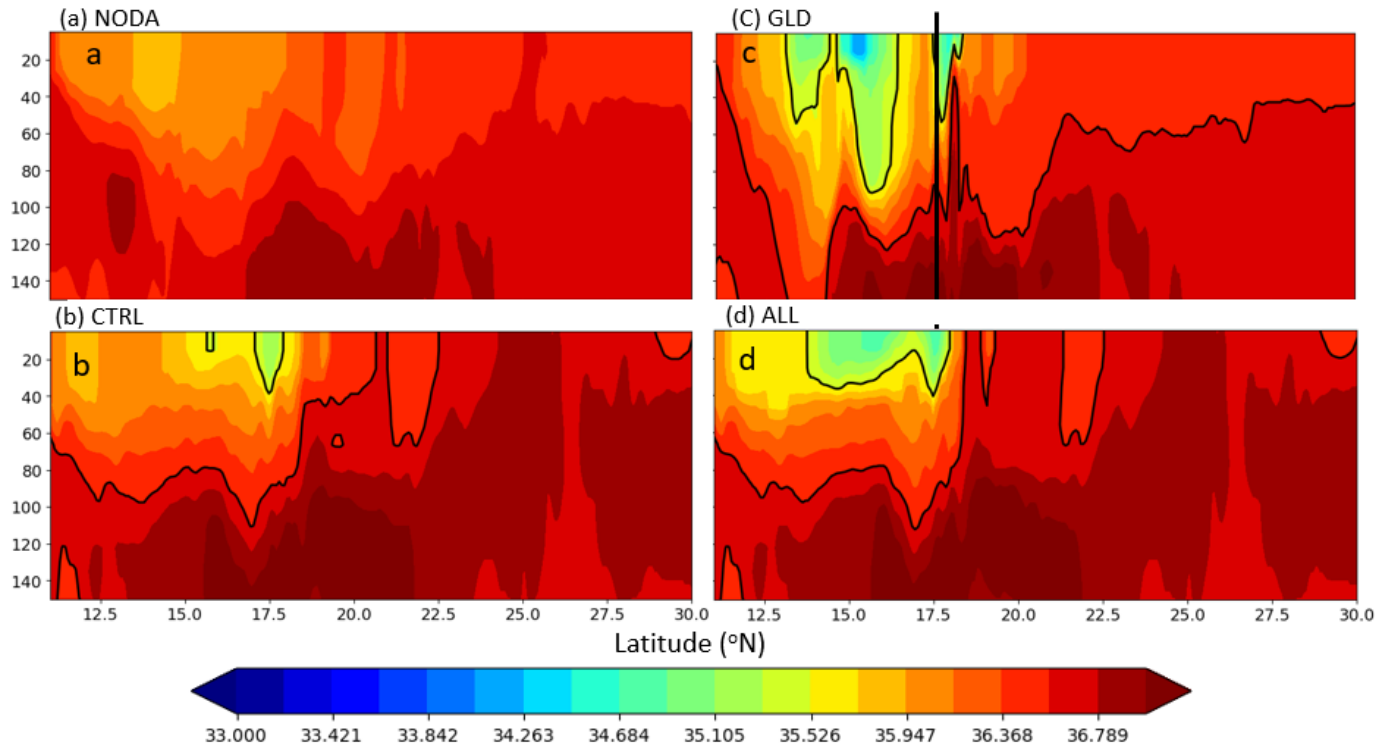

Figure 13. MOM6 Salinity distribution across 68oW latitudinal transection during pre-storm. (a) NODA; (b) CTRL; (c) GLD; (d) ALL. Black contour line indicates 35.5psu and 36.5psu isosalines.

Furthermore, we look at the time evolution of vertical salinity stratification on the left of the hurricane track at the Station SG663 (Figure 14). When glider observations are assimilated, the minimum salinity top 25m layer is captured by GLD and ALL during the data assimilation period at this location, which plays an important role of increasing vertical stratification and leading to the formation of the BLs. NODA and CTRL time series do not indicate this surface salinity minima and thus do not predict the proper upper ocean stratification and the BLs. In the presence of the BLs the increased salinity stratification within the isothermal layer reduces the vertical mixing caused by the hurricane and lead to increased SSTs warming on the left of the hurricane track.

File generated with AMS Word template 2.0

Accepted for publication in *Weather and Forecasting*. DOI 10.1175/WAF-D-22-0014.1.

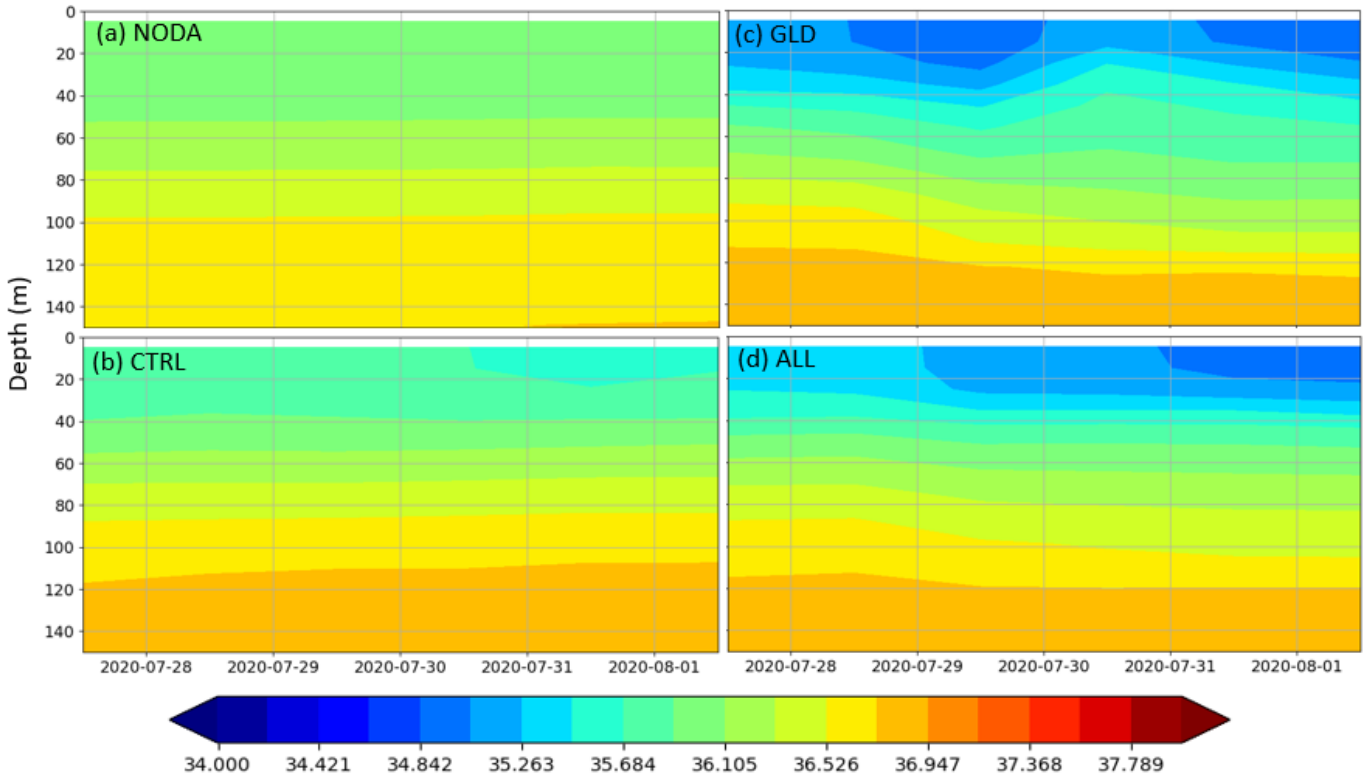

Figure 14. Time evolution of MOM6 vertical salinity stratification measured by SG663 during Hurricane Isaias. (a) NODA; (b) CTRL; (c) GLD; (d) ALL

On the right side of the hurricane track, derived from the ALL and GLD initial conditions, the observed salinity stratification at glider SG630's approximate location indicates vertical entrainment of deeper saline water at the surface in the beginning of the forecast period on July 28 and on July 30 (Figure 15), when the hurricane passes the 68°W latitudinal section. This results in deepening of 28°C isotherm and increased warm water entrainment form the pycnocline to the surface. As a result, an increased BLT develops (Figure 11). On July 30, Isaias advanced into a Category 1 hurricane instead of decaying, the increased vertical salinity entrainment and increases of the BLTs have provided an oceanic mechanism for its enhancement. CTRL initial condition does not indicate the vertical salinity entrainment throughout the forecast period, it also indicates a larger sub-surface salinity maximum at around 120m depth compared to the observation (Figure 11b).

File generated with AMS Word template 2.0

Accepted for publication in *Weather and Forecasting*. DOI 10.1175/WAF-D-22-0014.1.

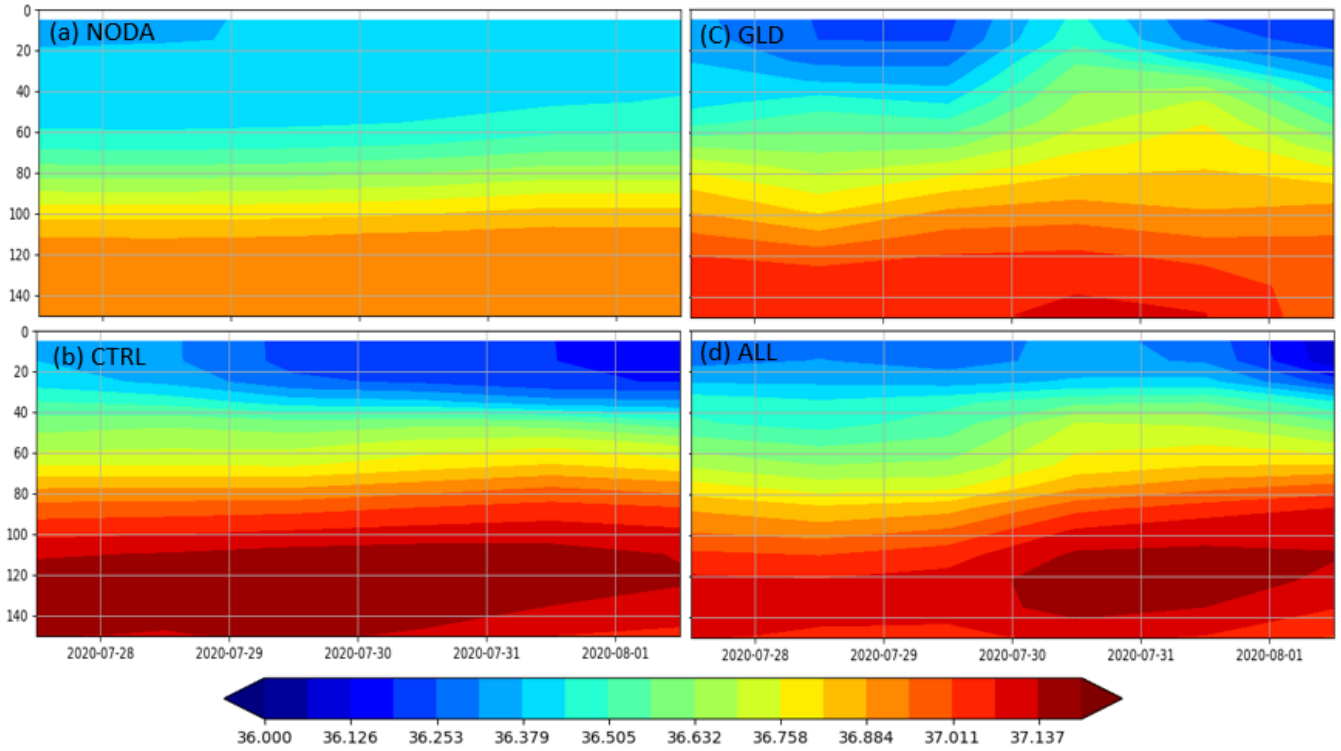

Figure 15. Time evolution of MOM6 vertical salinity stratification measured by SG630 during Hurricane Isaias. (a) NODA; (b) CTRL; (c) GLD; (d) ALL

When the BLTs are calculated and compared for four experiments within the model domain during the pre-storm), barrier layer thickness increases dramatically near where the glider observations are assimilated in GLD and ALL experiments (Figure 16c and 16d) comparing to NODA. The BLTs' increases in CTRL are not as prominent as GLD and ALL initial conditions when glider data are assimilated. In summary, during pre-storm there are increases in the BLTs from the left of the hurricane track to the further right of the track towards the north of the Puerto Rico Island near the 68°W longitudinal section when glider data are assimilated. Due to the fact that TC-induced cooling usually locates at the right side of the TC track in the northern hemisphere, the increased BLTs occurring to the right of Isaias' track in GLD and ALL initial conditions might have an effect of reducing the storm-induced cooling and even slight warming that help tropical storm Isaias march into a Category 1 hurricane. In order to prove this hypothesis, the enthalpy flux exchange and the SSTs changes during the hurricane forecast will be analyzed in Section 4b.

File generated with AMS Word template 2.0

Accepted for publication in *Weather and Forecasting*. DOI 10.1175/WAF-D-22-0014.1.

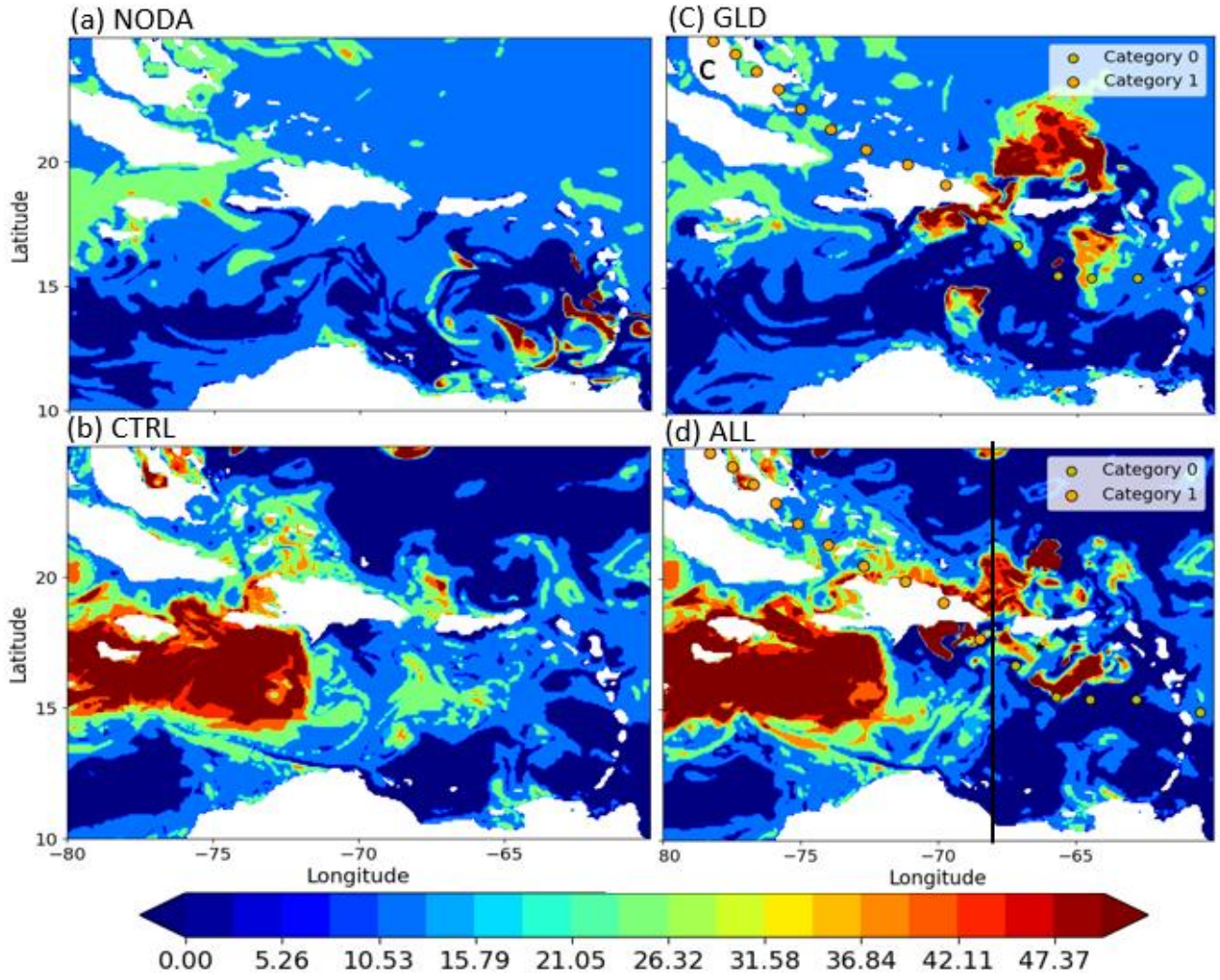

Figure 16. Pre-existing barrier layer thickness (m) for (a) NODA; (b) CTRL; (c) GLD; (d) ALL. Black star in (d) shows RUCOOL glider location to the right of Isaias' track. Black line indicates the location of the 68oW latitudinal transection.

Assimilating glider observations might also have an impact on the TCHP as an important indicator of hurricane intensification (Prasad and Hogan 2007). The initial TCHP conditions covering Isaias' 120-hour track are compared among the OHC calculations based on four initial conditions on July 28, 2020 in Figure 17. The minimum TCHP for a hurricane to occur is 50 KJ cm^{-2} with an optimal value of 60 KJ cm^{-2} (Mainelli et al 2008). NODA does not meet the minimum TCHP threshold for a hurricane to begin (i.e., mostly below 50 KJ cm^{-2} over the AWP). While GLD has the highest estimation of TCHP to the south and east of Puerto Rico island close to where glider observations are ingested, *i.e.,* > 80KJ cm^{-2}, CTRL shows a larger area of above 50KJ cm^{-2} TCHP to the north of Puerto Rico compared to GLD but below 80KJ cm^{-2} TCHP. Halliwell et al. 2015 shows that storms are usually more sensitive to TCHP than to their translation speed; for a hurricane with TCHP greater than 85KJ cm^{-2}, there is minimal ocean impact on its quasi-equilibrium intensity. In contrast, the TCHP

File generated with AMS Word template 2.0

Accepted for publication in *Weather and Forecasting*. DOI 10.1175/WAF-D-22-0014.1.

values in the adjacent of Isaias' track are mostly between 50 and 85KJ cm^{-2}, a bigger ocean's impact on hurricane intensity forecast should be expected for Isaias. Although assimilating glider data increases both the TCHP and BLTs in the adjacent of the Puerto Rico Island, the TCHP difference between CTRL and ALL is not as great as the BLTs, suggesting that the BLTs are more sensitive to glider data assimilation than the TCHP.

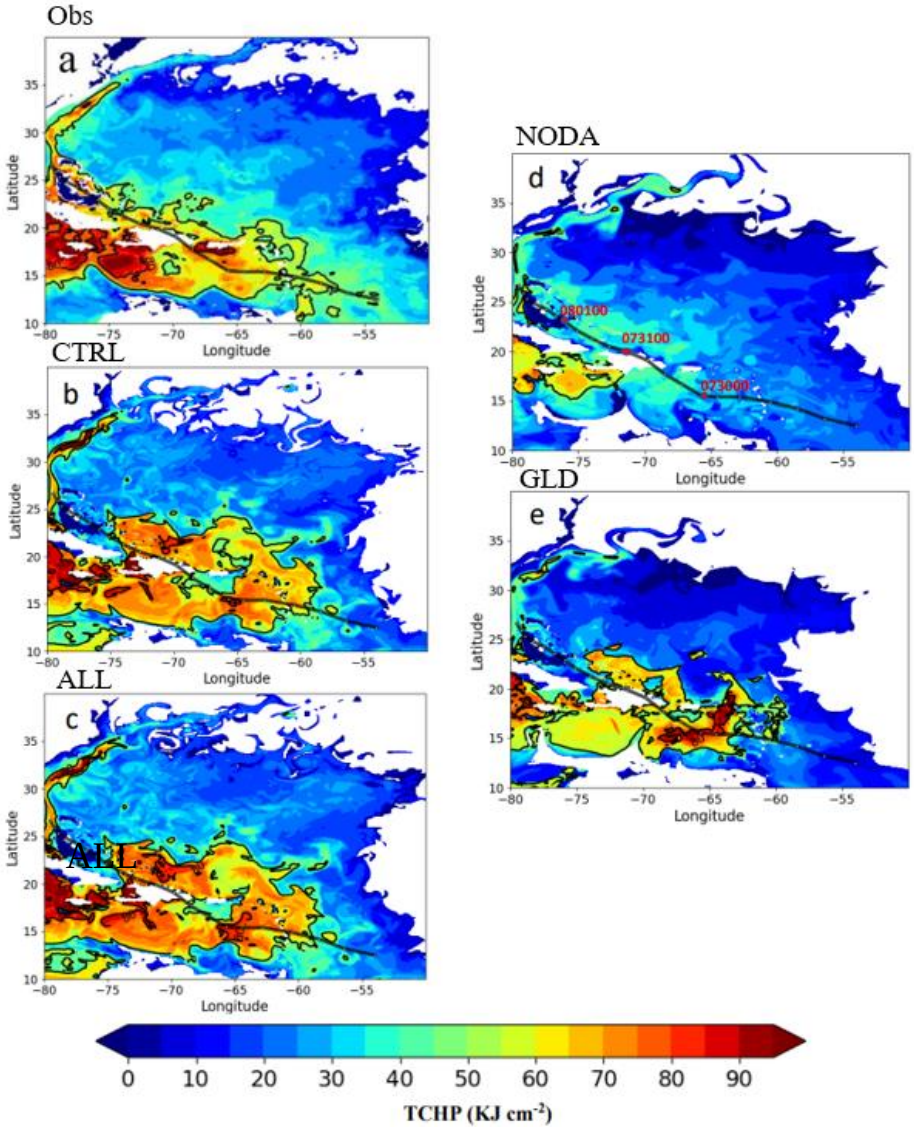

Figure 17. Tropical Cyclone Heat Potential (TCHP) near Isaias's track derived from (a) the Observation; (b) CTRL; (c) ALL (d) NODA; (e) GLD experiments on 28 July 2020. Contour lines indicate 50 and 80KJ cm-2 TCHP values. In (d), the dates are marked such that glider observations encountering Isaias' track are assimilated between 0000 UTC 30 July and 0000 UTC 31 July. Isaias intensifies into Category One hurricane between 0000 UTC 31 July and 1200 UTC 1 August.

4. Marine observations' impact on the forecast

a. impact on the ocean forecast

File generated with AMS Word template 2.0

Accepted for publication in *Weather and Forecasting*. DOI 10.1175/WAF-D-22-0014.1.

To assess marine observations' forecast impact, we analyze the along track ocean forecast errors compared to Operational Sea Surface Temperature and Sea Ice Analysis (OSTIA, https://podaac.jpl.nasa.gov/dataset/UKMO-L4HRfnd-GLOB-OSTIA) in Figure 18. In NODA, along track forecast errors are mostly negative with values greater than 0.6^{o}C between 20 and 85m depths (Figure 18a). Assimilating glider data clearly improves the along track forecast by reducing the error to below 0.2^{o}C in the first 78-h forecast (1200 UTC 29 July- 1800 UTC 1 August). Although slightly elevated, the along-track forecast errors during the last 42-h are also significantly reduced compared to NODA (Figure 18c). Assimilating satellite observations also reduces the along-track forecast error (Figure 18b). There are negative along track errors in the first 60-h forecast (i.e., 1200 UTC 29 July- 0000 UTC 1 August) and positive errors for the rest of the forecast hours (Figure 18b). In the CTRL initialized along track forecast, there are persistent negative errors (< 0.3^{o}C) between the 55th and 70th along track hours. It is not the case in the GLD and ALL initialized forecast, in which the forecast errors are reversed to become positive (below 0.3^{o}C) during similar along track forecast hours (i.e., approximately 60h- 80h). This result clearly indicates glider observation has impacts to either assimilating them alone (i.e., GLD experiment) or together with satellite observations (i.e., ALL).

Accepted for publication in *Weather and Forecasting*. DOI 10.1175/WAF-D-22-0014.1.

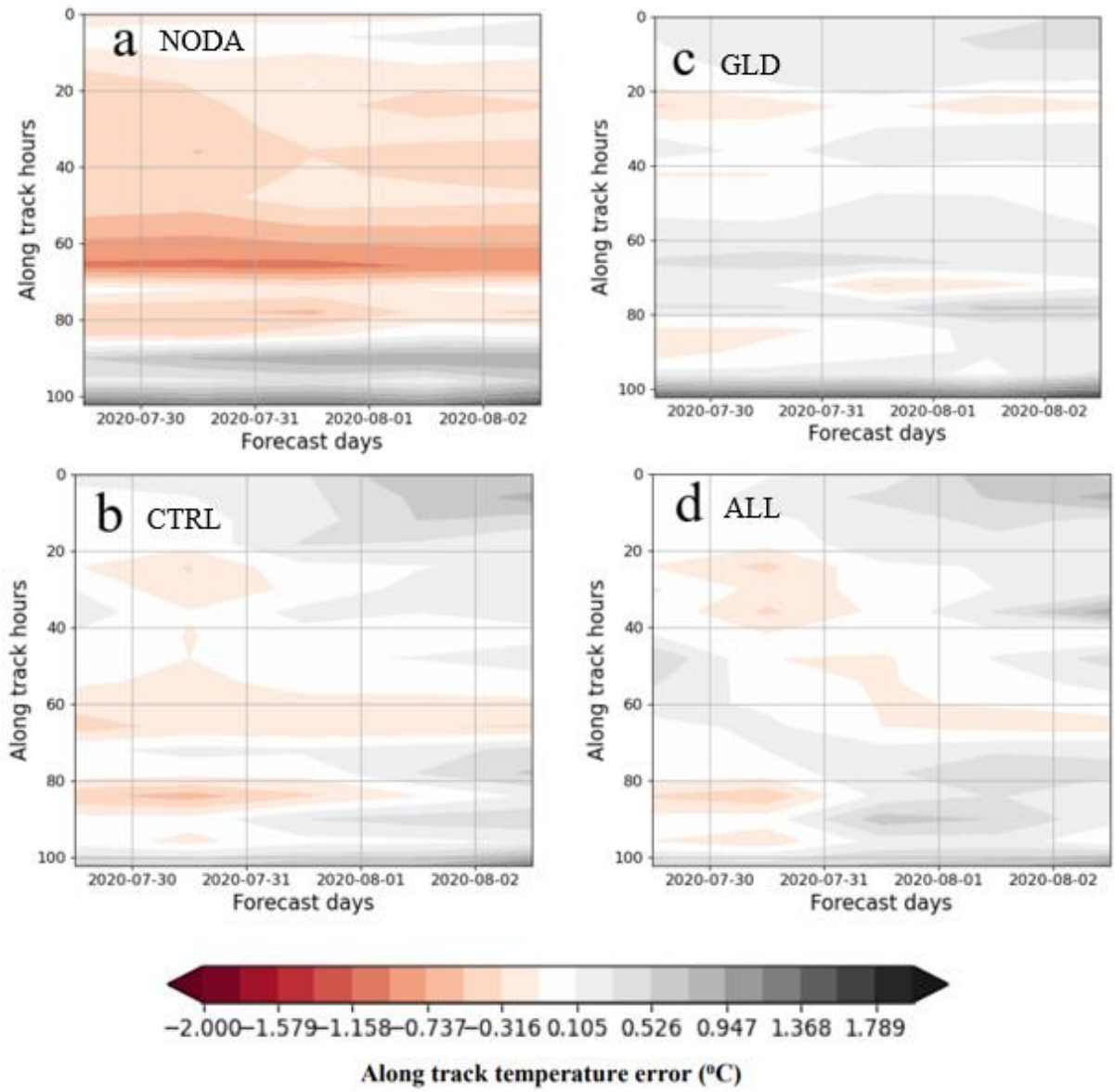

Figure 18. HAFS 120-hr forecast error of SSTs (1200 UTC 29 July – 1200 UTC 2 August, averaged between 28 and 29 July initial condition) initialized from four marine JEDI experiments (a) NODA; (b) CTRL; (c) GLD; (d) ALL, interpolated to along hurricane track and compared to satellite observation.

In order to quantify this impact, the statistics including the standard deviation, root mean square error and the correlation coefficient are shown by a Taylor diagram as well as the RMSD and correlation of the five-day forecast time series for four experiments (Figure 19). Assimilating satellite observations reduces the along-track RMSD by about 17% (i.e., $\frac{0.6-0.5}{0.6} \cdot 100\%$) compared to assimilating the glider data alone. There is additional 10% (i.e., $\frac{0.5-0.45}{0.5} \cdot 100\%$) of RMSD reduction on August 2, 2020 when glider data are assimilated in addition to

File generated with AMS Word template 2.0

Accepted for publication in *Weather and Forecasting*. DOI 10.1175/WAF-D-22-0014.1.

satellite observations (Figure 19b). Similar statistics is shown by the correlation coefficients (Figure 19c) although the increase of correlation for ALL compared to CTRL isn't as prominent as the RMSD reduction. Overall ocean forecast errors of along-track temperature in the 120-h HAFS forecasts are reduced the most by assimilating satellite and glider observations together (Figure 19a).

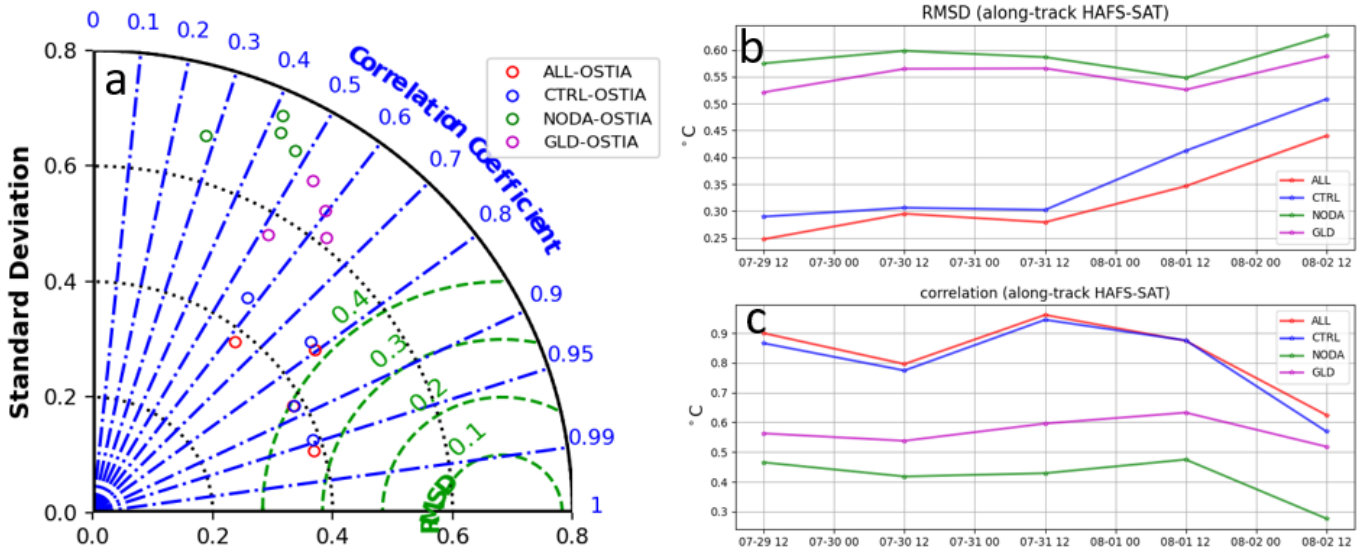

Figure 19. Statistical comparison of along-track HAFS 120-hr forecast error of SSTs initialized from four marine JEDI experiments. (a) Taylor diagram: different circles of same color stand for four subsequent forecast days (July 30-August 2, 2020); (b) Timer series of Root Mean Square Deviation; (c) Time series of correlation.

b. BLTs' impact on forecast enthalpy flux exchange and SSTs change

We have shown in Section 3b that the increased vertical entrainments of saline and warm water have increased the ILDs to the right of the hurricane track, which have contributed to the increased BLTs (up to 50m using 0.8°C temperature change criterion). Do the BLTs have an impact on forecasting SSTs cooling or hurricane intensification? In order to address these questions, we calculate the enthalpy flux at the air-sea interface (Figure 20), the SST changes (Figure 21) as well as the hurricane intensification factors from the HAFS forecasts initialized from four experiments (Table 2), and link them to the BLTs. First, the enthalpy flux exchange during pre-storm is analyzed as the sum of the latent and sensible heat fluxes initialized from four initial conditions. The increased enthalpy flux is mainly found to be located to the right of the hurricane track, where the major BLTs increases are located (Figure

File generated with AMS Word template 2.0

Accepted for publication in *Weather and Forecasting*. DOI 10.1175/WAF-D-22-0014.1.

16). Since TC-induced cooling mainly occurs near this location, this finding might indicate the SSTs cooling is suppressed in this area. Among four initial conditions, ALL shows the highest enthalpy flux transfer, followed by GLD initial condition. CTRL indicates moderate flux exchange while NODA shows minimum enthalpy flux exchange.

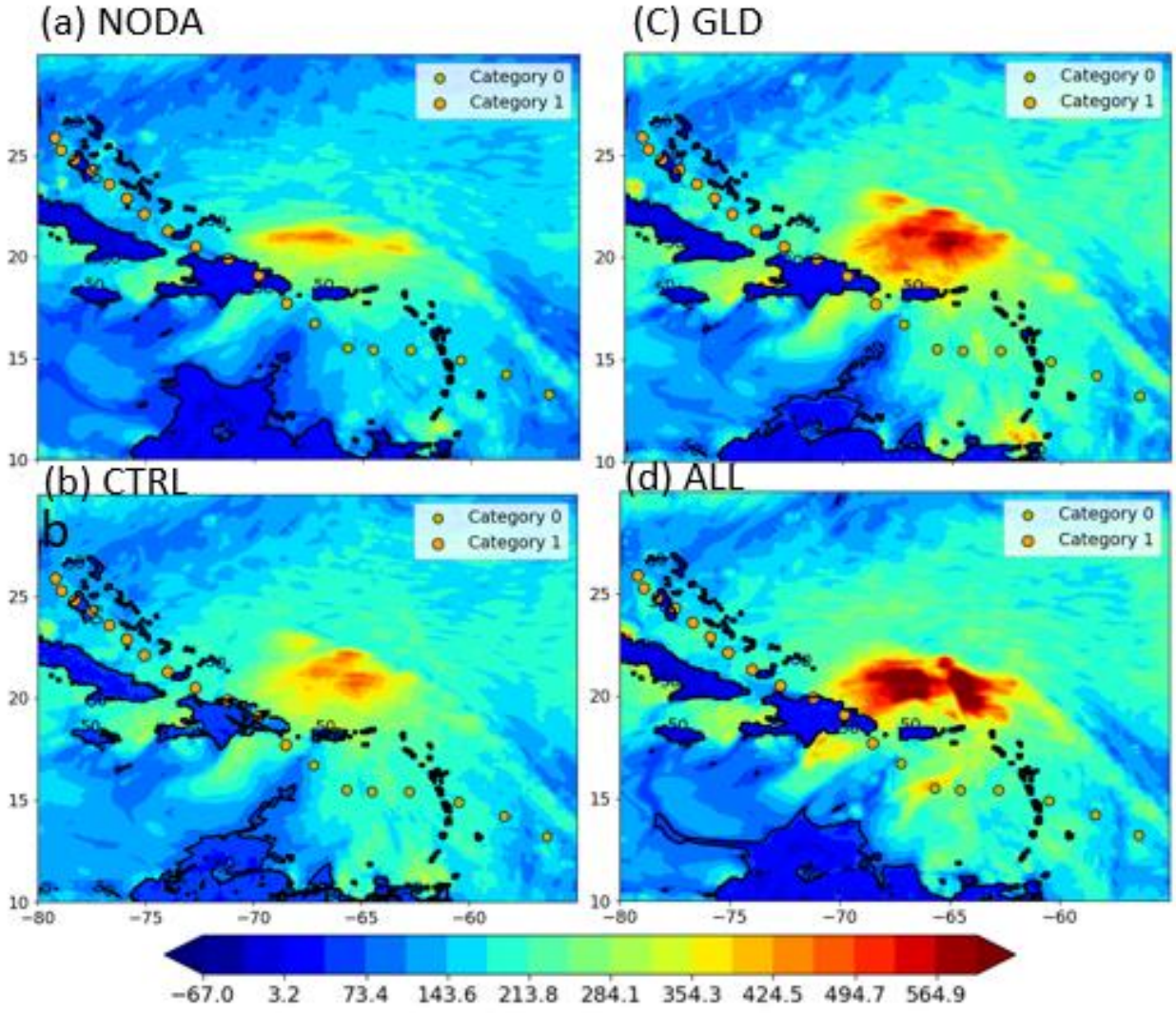

Figure 20. HAFS enthalpy flux (W m-2) on July 28, 2022. (a) NODA; (b) CTRL; (c) GLD; (d) ALL

Next, we try to address the question of "to which extent do these enthalpy flux transfers during the pre-storm affect the SSTs cooling?" by estimating the SSTs difference before and after the hurricane forecast period. The SSTs changes derived from HAFS forecasts initialized from ALL initial conditions indicate reduced SSTs cooling and even weak surface warming to the right of the hurricane track near 68^{o}W transection (Figure 21), coinciding with the location associated with the increased BLTs and euthalpy flix exchange in ALL

Accepted for publication in *Weather and Forecasting*. DOI 10.1175/WAF-D-22-0014.1.

initial condition shown by Figure 16d and 20d. GLD predicts the SSTs warming near 65°W to the right of the track, coinciding with the BLTs' increase locations in GLD initial condition (Figure 16c). CTRL predicts slight cooling on the right side of the hurricane track and slight warming on the left, consistent with the CTRL BLTs pattern shown by Figure 16b. NODA does not predict prominent cooling or warming on either side of the track. Therefore, we come at a conclusion that the reduced SSTs cooling and even warming on the right of the hurricane track is a result of reduced vertical mixing caused by increased BLTs, which leads to enhanced enthalpy flux as Hurricane Isaias passes this area.

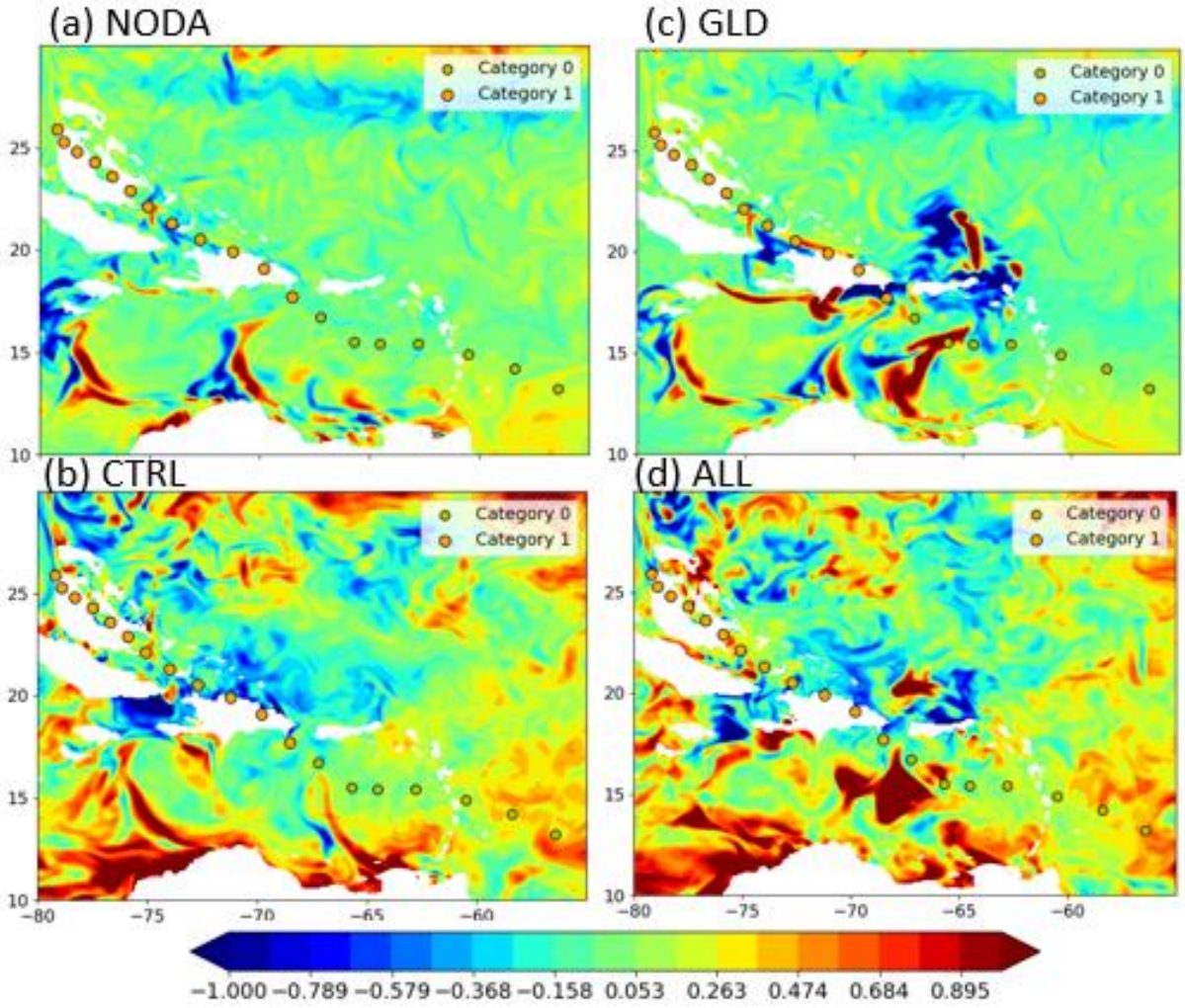

Figure 21. Forecast SSTs change (°C) between July 29 and August 2.

c. Hurricane Isaias forecast impact

File generated with AMS Word template 2.0

Accepted for publication in *Weather and Forecasting*. DOI 10.1175/WAF-D-22-0014.1.

The average 120-h Hurricane Isaias' track and intensity forecasts from 1200 UTC 28 July to 1200 UTC 2 August initialized by four JEDI experiments are shown by Figure 22. The 120-h forecast errors defined by the differences between the track and intensity using four initial conditions relative to the observation are shown by Figure 23. For the track forecast, although there are noticeable improvements for that lead by the ALL and GLD initial conditions, the differences among four predicted tracks for Isaias are relatively small comparing to the discrepancy between the observed and predicted tracks (Figure 23a). To examine ocean initial condition's impact on Isaias' intensity forecast, the 120-h minimum central pressure and maximum 10m wind are shown in Figure 22b and 22c. Without data assimilation ocean initial conditions, the NODA initialized forecast is not able to predict Isaias' intensification into a Category One hurricane - the maximum 10m wind is below 53 kts and minimum central pressure is above 995 hPa between 1200 UTC 28 July and 1800 UTC 1 August. Assimilating glider data helps GLD and ALL initial condition predict an intensified tropical storm with the maximum surface wind 60 kts and minimum central pressure 990 hPa. This result differs from that of Dong et al. 2017, in which there is little impact from the glider initialized intensity forecast for Hurricane Gonzalo. The difference is due to multiple factors. First, Isaias is a large hurricane (37-40km diameter) with relatively low TCHP (< 85KJ cm^{-2}), which provides larger distance and thus more time to adjust to local change of SSTs, this finding is supported by (Halliwell et al. 2015, their Figure 4); second, observations in this study are from six gliders with much broader spatial coverage (16.3-20.2^{o}N, 64-69^{o}W) compared to only one glider observations assimilated by Dong et al. 2017 (19.8-21.8^{o}N, 66-67^{o}W); last but not least important, this study found that assimilating glider data increases BLTs and mixes more saline and warm water from the pycnocline to the surface. This entrainment increases upper ocean stratification and suppressing vertical mixing and eventually leads to reduced storm-related cooling and even slight warming that help tropical storm Isaias march into a Category One hurricane.

Accepted for publication in *Weather and Forecasting*. DOI 10.1175/WAF-D-22-0014.1.

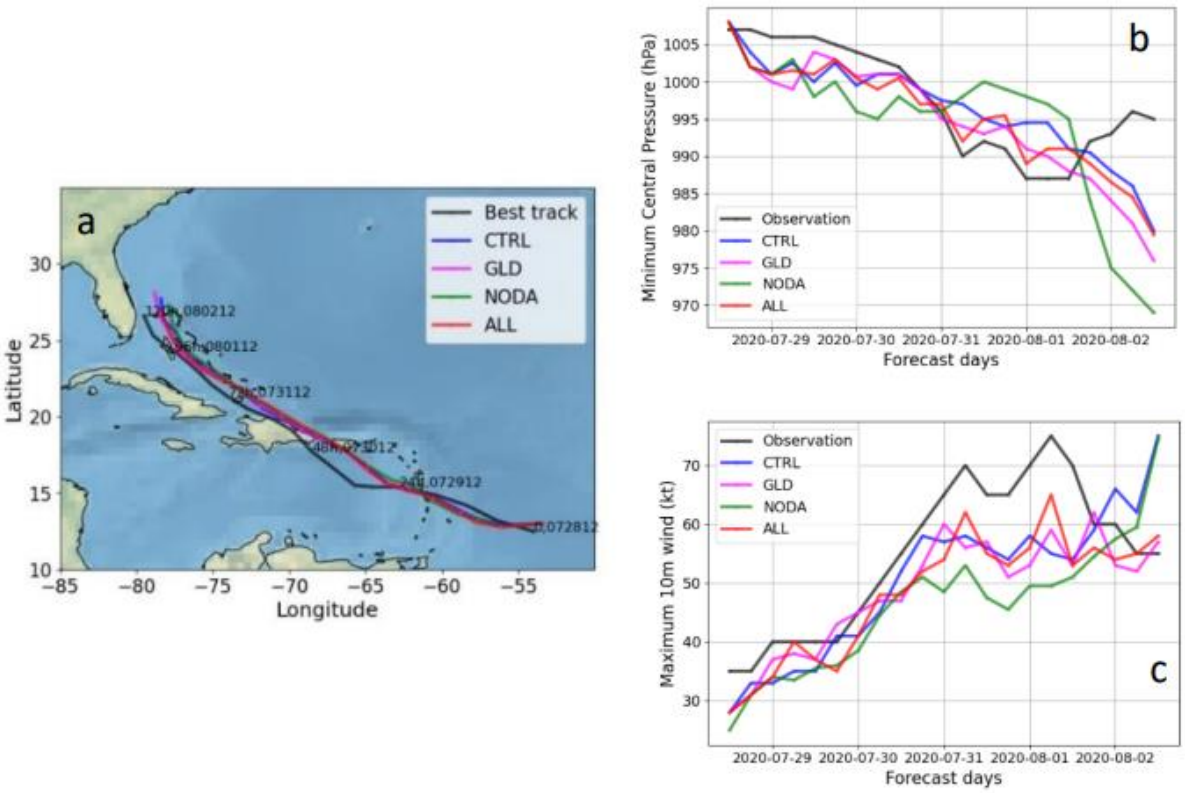

Figure 22. 120-hr HAFS forecast of Hurricane Isaias' (a) track; (b) minimum central pressure (hPa); (c) maximum 10m wind (kt) initialized from four experiments at 1200 UTC 28 July 2020 compared to the best track.

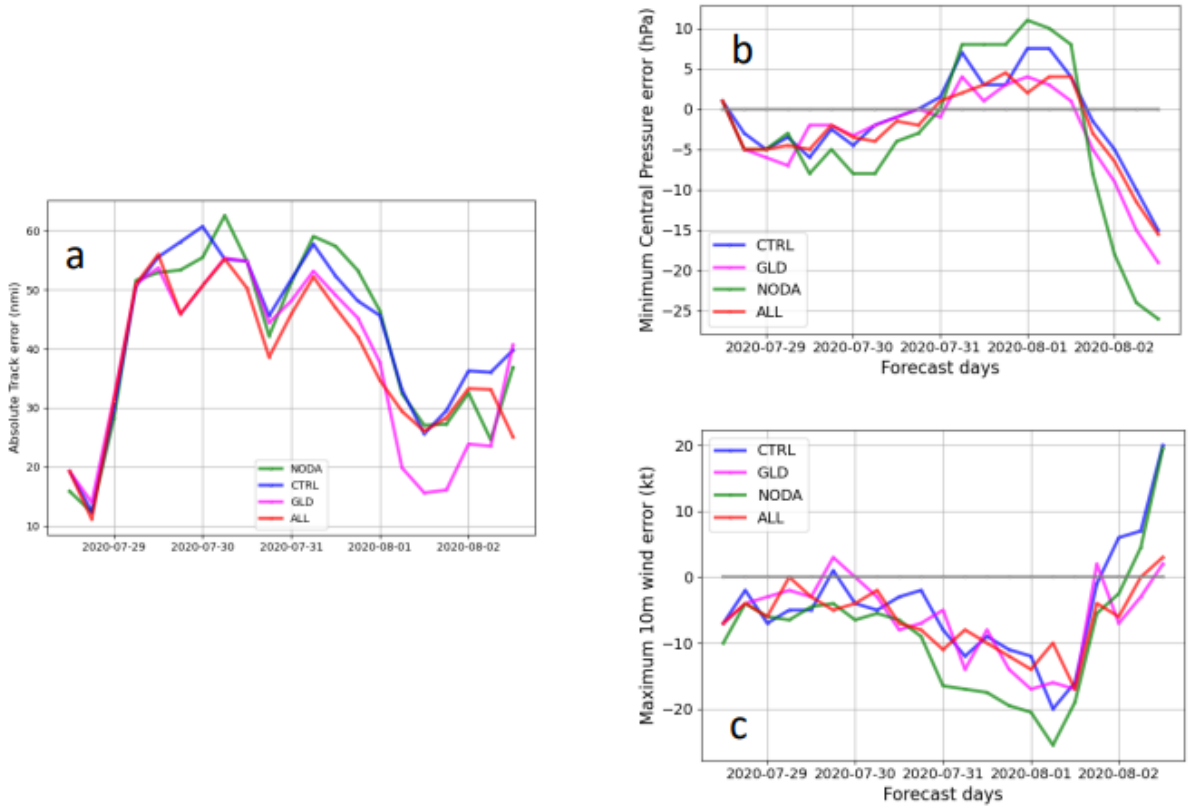

File generated with AMS Word template 2.0

Accepted for publication in *Weather and Forecasting*. DOI 10.1175/WAF-D-22-0014.1.

Figure 23. HAFS 120-hr forecast error for Hurricane Isaias' (a) track (nmi); (b) minimum central pressure (hPa); (c) maximum 10m wind (kt) initialized from four experiments at 1200 UTC 28 July 2020 compared to the best track.

To summarize the performances of hurricane intensity forecast initialized by four experiments, we calculate the correlation coefficient, standard deviation and RMSD normalized by the maximum wind and minimum pressure departure from the observation and show the statistics in the following Taylor diagrams (Figure 24). For the minimum pressure, ALL has improved standard deviation by 10% ($\frac{0.33-0.3}{0.3} \cdot 100\%$) compared to CTRL when it is compared to the observation. Both CTRL and ALL show improved RMSDs by 15% ($\frac{0.4-0.35}{0.4} \cdot 100\%$) compared to GLD. GLD shows higher correlation with the observation, smaller RMSD and standard deviation compared to NODA. For the maximum 10m wind, ALL initial condition leads the RMSD statistics by 7% ($\frac{0.31-0.29}{0.29} \cdot 100\%$), 20% ($\frac{0.35-0.29}{0.29} \cdot 100\%$), 40% ($\frac{0.41-0.29}{0.29} \cdot 100\%$) compared to GLD, CTRL and NODA initial conditions.

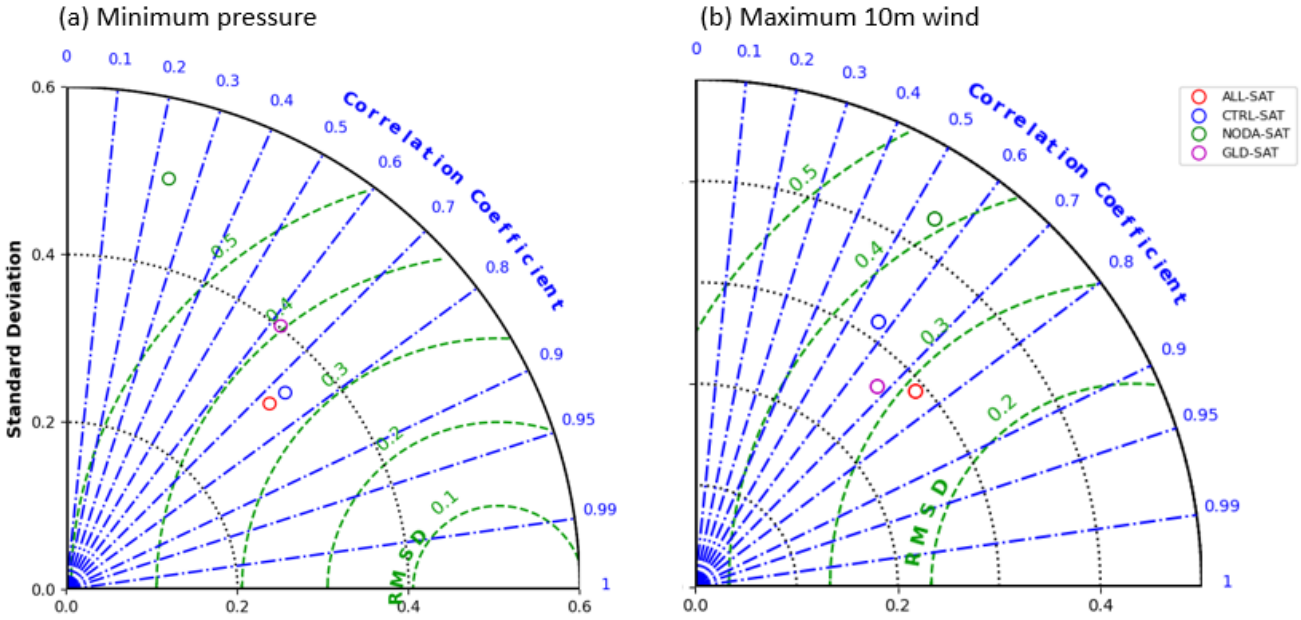

Figure 24. Taylor diagrams for (a) minimum pressure and (b) maximum 10m wind, normalized by maximum pressure and 10m wind difference with respect to observation.

We also calculated the forecast hurricane intensification factors for four initial conditions using a linear regression approach for the maximum wind speed and show comparison

File generated with AMS Word template 2.0

Accepted for publication in *Weather and Forecasting*. DOI 10.1175/WAF-D-22-0014.1.

between four initial conditions and the observation (Table 2). All four initial conditions underestimate the intensification factors when compared to the observations, with the percentages of the underestimation being 45%, 34%, 37%, 16% for NODA, GLD, CTRL and ALL, respectively. ALL initial condition leads to the closest intensification factor compared to the observation, followed by GLD initial condition. NODA leads to the largest underestimation. ALL enhances the forecast intensification factor by 24% (i.e., $\frac{1.54-1.17}{1.54} \cdot 100\%$) comparing to CTRL. Combining the statistics shown by Figure 24 and the intensification factors shown by Table 2, ALL initial condition assimilating glider and satellite observations is proven to improve the robustness and strength of the hurricane intensity forecast.

Initial conditions	NODA	GLD	CTRL	ALL	OBS
Intensification factors	1.01	1.21	1.17	1.54	1.85

Table 2. HAFS forecast Intensification factors (m s-1 per 36 hours) from four initial conditions compared to the observation.

5. Discussion and conclusion

The goal of this study is to understand the impact of assimilating marine observations including satellite observations and underwater hurricane glider data on initializing ocean and hurricane forecast using a high-resolution atmospheric-oceanic coupled system. During the pre-storm, Marine JEDI data assimilation has led to improvements of the initial upper ocean temperature and salinity structure compared to the case without data assimilation. The assimilation of satellite observations in marine JEDI has shown 25% of improvement for the upper-ocean temperature initial condition and 42% of improvement for the upper-ocean salinity initialization. Assimilating glider data in addition to satellite observations further improve the surface temperature and salinity by 30% and 8%, respectively. Underwater hurricane gliders provide detailed information about the upper-ocean conditions which helps us understand the ocean's critical role in hurricane initialization and intensification. The improved salinity initial condition when glider data are assimilated has led to a more accurate prediction of the upper-ocean stratification that creates a barrier layer suppressing SST

Accepted for publication in *Weather and Forecasting*. DOI 10.1175/WAF-D-22-0014.1.

cooling during the pre-storm. Assimilating glider observations also has an impact on the TCHP as an important indicator of hurricane intensification. As estimated by Mainelli et al. 2008, the optimal threshold for a hurricane to maintain is approximately 50 KJcm^{-2}, with the optimal value being 60 KJcm^{-2}. The locations of the 50 and 80 KJcm^{-2} TCHPs indicate that without assimilating glider and satellite observations the model fails to predict the correct pre-storm heat potential for Hurricane Isaias to develop. Assimilating glider and satellite observations is essential to predict the correct TCHP for Isaias to intensify from a tropical storm into a Category One hurricane. Although assimilating glider data increases both the TCHP and BLTs in the adjacent of the Puerto Rico Island, the TCHP change assimilating glider data in additional to satellite observations is not as great as the BLTs, suggesting that the BLTs are more sensitive to glider data assimilation than the TCHP.

The role of a salinity-induced barrier layer on hurricane intensification within the upper ocean is evaluated. Previous studies demonstrate salinity stratified barrier layers in the tropical ocean can significantly impact hurricane intensification (Balaguru et al. 2012). Compared among four ocean initial conditions, we show that when satellite and glider observations are both assimilated, the ILDs deepen especially to the right of the hurricane track, where storm-induced cooling usually occurs in the northern hemisphere. By definition this phenomenon leads to increased BLTs. During pre-storm there are increases in the BLTs from the left of the hurricane track to the further right of the track towards the north of the Puerto Rico Island near the 68^{o}W longitudinal section when glider data are assimilated. The increased BLTs in initial conditions assimilating glider data have an effect on entraining saline and warm water from the pycnocline to the near surface, which increase upper ocean stratification and suppress vertical mixing. It eventually leads to reduced storm-related cooling and even slight warming. The BLTs increase ultimately leads to increased air-sea enthalpy flux exchange and reverses sea surface temperature cooling. This mechanism also lasts beyond the pre-storm shown by the time evolution of the vertical stratification and have become one of the major mechanisms that Isaias advanced from a tropical storm into a Category One hurricane. In order to demonstrate this effect on hurricane intensification, we show the forecast SSTs changes derived from four initial conditions before and after the hurricane forecast period. The results indicate larger SSTs changes are associated with increased BLTs and enthalpy flux transfers. Meanwhile increased BLTs are also associated with increased hurricane intensification factor and reduced intensity forecast error. BLT's response pattern to glider data assimilation is further demonstrated by the vertical

Accepted for publication in *Weather and Forecasting*. DOI 10.1175/WAF-D-22-0014.1.

stratification of 68ºW latitudinal vertical section across the hurricane track. When glider data are assimilated, on the left of the hurricane track the depth of mixing layer depth increases by nearly two folds, there is also a warm and low-salinity storm water discharge that increases upper ocean stratification and reduces hurricane induced vertical mixing and thus plays an important part for the SSTs warming; on the right of the hurricane track the 28ºC isotherm deepens, leading to increased BLTs.

As a result of improved BLTs during initialization, the forecast hurricane intensity error is found reduced when the initial condition assimilates both satellite and glider data. There is up to 10% of improvement in its statistics compared to the initial condition assimilating only satellite observations. Furthermore, we calculate the hurricane intensification factor using a linear regression approach for four initializations and our results indicate the closest intensification factor to the observation happens when both data type are used in the ocean initialization experiments. Using either satellite or glider observation leads to larger intensification factor compared to no data assimilation initial condition, but the intensification impact isn't as large as when both data types are assimilated together, which leads to up to 24% of enhancement of the intensification factor compared to only assimilate satellite observations. Since Hurricane Isaias has caused the most devastating losses since Hurricane Sandy, the amount of improvement in hurricane intensity forecast would at least prepare the local community for evacuation and property protection that ultimately minimizes property losses and protect lives. This study provides evidence in favor of the theory that the ocean serves as a massive entropy source that supports hurricane intensification, and has demonstrated that the ocean initialization of hurricane forecast assimilating comprehensive marine observations is essential to an accurate estimation of hurricane intensity forecast.

As part of the Unified Forecast System (UFS), the mediator coupling using CDEPS between HAFS and JEDI SOCA provides the technical basis for this study. However, the coupling which happens only at the sea surface limits our scope of the full feedback between the ocean and a typical hurricane. For instance, the hurricane intensity forecast has a negative bias during most of the forecast period, which could be attributed to the lack of three-dimensional ocean coupling. Despite of the limitations, this study has demonstrated the mechanisms of an improved ocean initial condition and its impact on hurricane forecast through assimilating comprehensive marine observations under a unified JEDI-HAFS forecast system.

File generated with AMS Word template 2.0

Accepted for publication in *Weather and Forecasting*. DOI 10.1175/WAF-D-22-0014.1.

Acknowledgments.

Hurricane Supplemental at NOAA/NCEP/NWS/EMC and NOAA/NOS/CO-OPS provided main funding resource for this research.

Mississippi State University Orion super computer provides computing resource for most of the findings presented in this manuscript.

Data Availability Statement.

This manuscript is supported by multiple datasets. Underwater glider data used in this manuscript are openly available from NOAA/AOML and IOOS. These datasets can accessed from the following public domain (https://www.aoml.noaa.gov/phod/goos/gliders/data.php And, https://data.ioos.us/thredds/dodsC/deployments/); Absolute Dynamic Topography data used for assimilation can be accessed from the following ftp site of NESDIS RADS (ftp://ftp.star.nesdis.noaa.gov/pub/sod/lsa/rads/adt); Sea Surface Temperature data from VIIRS, GMI, WindSat, AMSR2 used for assimilation in this study can be accessed through the PODAAC (login required) (https://podaac-tools.jpl.nasa.gov/drive/files/allData/ghrsst/data/GDS2/ and,

ftp://ftp.star.nesdis.noaa.gov/pub/socd2/coastwatch/sst/ran/viirs/npp/l3u); Satellite SST observations used for model verification can be accessed through: https://podaac.jpl.nasa.gov/dataset/UKMO-L4HRfnd-GLOB-OSTIA; Best hurricane track data can be found openly through NOAA NHC (https://www.nhc.noaa.gov/data/#hurdat)

REFERENCES

Adcroft, A., W. G. Anderson, V. Balaji, C. Blanton, M. Bushuk, C. O. Dufour, J. P. Dunne, S. M. Griffies, R. Hallberg, M. J. Harrison, I. M. Held, M. Jansen, J. G. John, J. P. Krasting, A. R. Langenhorst, S. Legg, Z. Liang, C. McHugh, A. Radhakrishnan, B. G. Reichl, A. Rosati, B. L. Samuels, A. Shao, R. J. Stouffer, M. Winon, A. T. Wittenberg, B. Xiang, N. Zadeh and R. Zhang, 2019: The GFDL Global Ocean and Sea Ice Model OM4.0: Model Description and Simulation Features. Journal of Advances in Modeling Earth Systems, 11(10), DOI: 10.1029/2019MS001726.

File generated with AMS Word template 2.0

Accepted for publication in *Weather and Forecasting*. DOI 10.1175/WAF-D-22-0014.1.

Balaguru, K., P. Chang, R. Saravanan, R. Leung, Z. Xu, M. Li, and J. S. Hsieh, 2012: Ocean barrier layers' effect on tropical cyclone intensification. Proc Natl Acad Sci U S A. 2012 Sep 4;109(36):14343-7. doi: 10.1073/pnas.1201364109.

CDEPS documentation: https://escomp.github.io/CDEPS/html/index.html

Chang, S. W., 1979: The response of an axisymmetric model tropical cyclone to local variations of sea surface temperature. Monthly Weather Review, 107, 662–666.

Chelton, D. B., R. A. de Szoeke, M. G. Schlax, K. El Naggar and N. Siwertz, 1998: Geographic variability of the first baroclinic Rossby radius of deformation. J. Phys. Oceanogr., 28, 433–460, https://doi.org/10.1175/1520-0485(1998)028,0433: GVOTFB.2.0.CO;2.

Courtier, P., E. Andersson, W. Heckley, J. Pailleux, D. Vasiljevic, M. Hamrud, A. Hollingsworth, F. Rabier and M. Fisher, 1998: The ECMWF implementation of three-dimensional variational assimilation (3D-Var). I: Formulation. Quarterly Journal of the Meteorological Society. (1998), 124, pp. 1783-1807

Dickey, T., D. Frye, J. McNeil, D. Manov, N. Nelson, D. Sigurdson, H. Jannasch, D. Siegel, T. Michaels, and R. Johnson, 1998: Upper-Ocean Temperature Response to Hurricane Felix as Measured by the Bermuda Testbed Mooring. Mon. Wea. Rev., 126, 1195-1201.

Domingues, R., G. Goni, F. Bringas, S. Lee, H. Kim, G. Halliwell, J. Dong, J. Morell, and L. Pomales, 2015: Upper ocean response to Hurricane Gonzalo (2014): Salinity effects revealed by targeted and sustained underwater glider observations. Geophysical Research Letters 42, 7131–7138.

Dong, J., R. Domingues, G. Goni, G. Halliwell, H-S. Kim, S-K. Lee, M. Mehari, F. Bringas, J. Morell and L. Pomales, 2017: Impact of Assimilating Underwater Glider Data on Hurricane Gonzalo (2014) Forecasts. Weather and Forecasting, 2017; 32 (3): 1143.

Emanuel, K. A., 1991: The Theory of Hurricanes. Ann. Rev. Fluid Mech. 23: 179-96.

Emanuel, K. A., C. DesAutels, C. Holloway, R.L. Korty, 2004: Environmental control of tropical cyclone intensity. J. Atmos. Sci. 61:843–858.

Glenn, S. M., T. N. Miles, G. N. Seroka, Y. Xu, R. K. Forney, F. Yu, H. Roarty, O. Schofield, and J. Kohut, 2016: Stratified coastal ocean interactions with tropical cyclones. Nature Communications 7. Article number: 10887.

Accepted for publication in *Weather and Forecasting*. DOI 10.1175/WAF-D-22-0014.1.

Goni, G., M. DeMaria, J. Knaff, C. Sampson, I. Ginis, F. B. A. Mavume, C. Lauer, I.-I. Lin, M. M. Ali, P. Sandery, S. Ramos-Buarque, K. Kang, A. Mehra, E. Chassignet, and G. Halliwell, 2009: Applications of satellite-derived ocean measurements to tropical cyclone intensity forecasting. Oceanography, 22**,** 190-197.

Halliwell., G. R., L.K. Shay, S.D. Jacob, O.M. Smedstad and E.W. Uhlhorn, 2008: Improving ocean model initialization for coupled tropical cyclone forecast models using GODAE nowcasts Monthly Weather Review: 2576-2591.

Halliwell, G. R., Jr., A. Srinivasan, V. Kourafalou, H. Yang, D. Willey, M. L. Hénaff, and R. Atlas, 2014: Rigorous evaluation of a fraternal twin ocean OSSE system for the open Gulf of Mexico. Journal of Atmospheric Oceanic Technology, 31, 105–130.

Halliwell, G. R., S. Gopalakrishnan, F. Marks, and D. Willey, 2015: Idealized study of ocean impacts on tropical cyclone intensity forecasts. Mon. Wea. Rev., 143, 1142–1165, doi:10.1175/ MWR-D-14-00022.1.

James R. Holton, 2004: An Introduction to Dynamic Meteorology (Fourth edition).

JEDI Documentation: https://jointcenterforsatellitedataassimilation-jedi-docs.readthedocs-hosted.com/en/latest/index.html

Kara, A. B., P.A. Rochford, and H. E. Hurlburt, 2000: Mixed layer depth variability and barrier layer formation over the north Pacific Ocean. Journal of Geophysics Research, 105, 16783-16801.

Kleist, D. T., D. F. Parrish, J. C. Derber, R. Treadon, R. M. Errico and R. Yang, 2008: improving Incremental Balance in the GSI 3DVAR Analysis System. Monthly Weather Review, 137: DOI: 10.1175/2008MWR2623.1.

Kurapov, A., J. Xu, Z. Burnett, E. Myers, E. Bayler, I. Pasmans, A. Moore and H. Arango, 2018: Data Assimilation in the US West Coast Ocean Forecast System (WCOFS). PDF available at: https://www.godae.org/~godae-data/OceanView/Events/COSS-TT-2018/2.4-20180919_godae_coss_tt_kurapov.pdf

Leipper, D. F., and D. Volgenau, 1972: Hurricane heat potential of the Gulf of Mexico, J. Phys. Oceanogr., 2, 218 – 224.

Liu, B., H. Kim, D. Rosen, J. Dong, B. Thomas, D. Sheinin, Z. Zhang, H. Winterbottom, L. Zhu, C. Zhang, W. Wang, J. Shin, D. Iredell, K. Wu, R. Dunlap, A. Mehra and V.

Accepted for publication in *Weather and Forecasting.* DOI 10.1175/WAF-D-22-0014.1.

Tallapgrada, 2020: A Stand-Alone Regional and Ocean-Coupled HAFS for Hurricane Forecasting in the North Atlantic Basin. UFS Users Workshop, July 28, 2020.

Lloyd, I. and G. A. Vecchi, 2011: Observational evidence for oceanic controls on hurricane intensity. Journal of climate. Volume 24, Issue 4. Page(s): 1138–1153.

Mainelli, M., M. DeMaria, L. K. Shay, and G. Goni, 2008: Application of oceanic heat content estimation to operational forecasting of recent Atlantic category 5 hurricanes. Weather and Forecasting, DOI: https://doi.org/10.1175/2007WAF2006111.1

Mellor, G. L. and T. Ezer, 1991: A Gulf Stream Model and and Altimetry Assimilation Scheme. Journal of Geophysical Research, Vol. 96. NO. C5, Pages: 8779-8795.

Mourre, B., and J. Chiggiato, 2014: A comparison of the performance of the 3-D super ensemble and an ensemble Kalman filter for short-range regional ocean prediction. Tellus A, doi:10.3402/tellusa.v66.21640

National Weather Service, Hurricane Isaias 2020: https://www.weather.gov/ilm/HurricaneIsaias2020

Oke, P. R., P. Sakov, and E. Schulz, 2009: A comparison of shelf observation platforms for assimilation in an eddy-resolving ocean model, Dynamics of Atmospheres and Oceans, Volume 48, Issues 1–3, 121-142.

Pauluis, O.M. and F. Zhang, 2017: Rconstruction of Thermodynamic Cycles in a High-Resolution Simulation of a Hurricane. Journal of the Atmospheric Sciences, DOI: https://doi.org/10.1175/JAS-D-16-0353.1. Page(s): 3367–3381.

Pielke, RA, Jr, J. Rubiera, C. Landsea, ML. Fernandez, R. Klein, 2003: Hurricane vulnerability in Latin America and the Caribbean: Normalized damage and loss potentials. Nat. Hazards Rev. 4:101–114.

Prasad, T. G. and P. J. Hogan, 2007: Upper-ocean response to Hurricane Ivan in a 1/25 nested Gulf of Mexico HYCOM. Journal of Geophysical research, Vol. 112, C04013.

Press, W. H., W. T. Vetterling, S. A. Teukolsky, B. P. Flannery, 1992: *Numerical Recipes in C, Second Edition*. Cambridge University Press.

Shay, L. K., G. J. Goni, and P. G. Black, 2000: Effects of warm oceanic feature on Hurricane Opal, Mon. Weather Rev., 128, 1366– 1383.

Accepted for publication in *Weather and Forecasting*. DOI 10.1175/WAF-D-22-0014.1.

Tallapragada, V., L. Bernardet, M. Biswas, I. Ginis, Y.Kwon, Qingfu Liu, T. Marchok, D. Sheinin, B. Thomas, Mingjing Tong, S. Trahan, W. Wong, R. Yablonsky, Xuejin Zhang, 2015: Hurricane Weather Research and Forecasting (HWRF) model: 2015 scientific documentation. Developmental Testbed Center: http://www.dtcenter.org/HurrWRF/users/docs/scientific_documents/HWRF_v3.7a_SD.pdf

Testor, P., B. D. Young, D. L. Rudnick, S. Glenn, D. Hayes, C. M. Lee, C. Pattiaratchi, K. Hill, A. Mehra, et al. 2019: OceanGliders: A Component of the Integrated GOOS. Frontiers in Marine Science, 02 October 2019, https://doi.org/10.3389/fmars.2019.00422

Trémolet, Y., and T. Auligné, 2020: The Joint Effort for Data Assimilation Integration (JEDI). JCSDA Quart., No. 66 (winter 2020), Joint Center for Satellite Data Assimilation Office, College Park, MD, 1–5, https://doi.org/10.25923/ rb19-0q26.

Verfahrenstechnik, VDI-Gesellschaft, Chemieingenieurwesen, 2005: VDI Heat Atlas. Springer-Verlag Berlin-Heidelberg.

Wang, C., and S.-K. Lee, 2007: Atlantic warm pool, Caribbean lowlevel jet, and their potential impact on Atlantic hurricanes. Geophys. Res. Lett., 34, L02703.

Wang, X., G. Han, Y. Qi, and W. Li, 2011: Impact of barrier layer on typhoon-induced sea surface cooling. Dyn. Atmos. Oceans, 52, 367–385.

Wikipedia article on Hurricane Isaias. https://en.wikipedia.org/wiki/Hurricane_Isaias

File generated with AMS Word template 2.0

Accepted for publication in *Weather and Forecasting.* DOI 10.1175/WAF-D-22-0014.1.